

REPUBLIC OF AZERBAIJAN

On the rights of the manuscript

ABSTRACT

of the dissertation for the degree of Doctor of Science

**HOPPING MECHANISMS OF PHASE TRANSITIONS AND
CHARGE TRANSPORT OF ABX_2 (WHERE $A=Cu, Tl$; $B=Fe,$
 Cr, Co, Ni, Ga, In ; $X=S, Se, Te$) TYPE LOW-DIMENSIONAL
SEMICONDUCTORS**

Speciality: 2222.01 – Semiconductor Physics

Field of Science: Physics

Applicant: **Aydin Ismayil Jabbarov**

Baku – 2022

The dissertation work was performed at the "Resonance Phenomena in Solids" laboratory of the Institute of Physics of Azerbaijan National Academy of Sciences.

Official Opponents: Doctor of Physics and Mathematics Sciences,
Professor

Karim Rahim Allahverdiyev

Doctor of Physics and Mathematics Sciences,
Associate Professor

Nadir Allahverdi Abdullayev

Doctor of Physics and Mathematics Sciences,
Professor

Rauf Madat Sardarli

Doctor of Physics and Mathematics Sciences,
Professor

Hamza Samad Seyidli

Dissertation council ED 1.14 of Supreme Attestation Commission under the President of the Republic of Azerbaijan operating at Institute of Physics of Azerbaijan National Academy of Sciences

Chairman of the Dissertation council:

Active member of ANAS, Doctor of Physics and Mathematics Sciences, Professor

Nazim Timur Mammadov

Scientific secretary of the dissertation council:

Doctor of Physics Sciences, Associate Professor
Rafiq Zabil Mehdiyeva

Chairman of the scientific seminar:

Doctor of Physics and Mathematics Sciences,
Associate Professor

Talat Rzagulu Mehdiyev

GENERAL DESCRIPTION OF WORK

Relevance of the topic and degree of elaboration:

Phase transitions are one of the most widespread and interesting phenomena, both in fundamental scientific research and in technological applications. The theory, which describes the main aspects of the physics of phase transitions was given by L.D. Landau. The main point of Landau's theory is the concept of the order parameter- a quantity equal to zero in the disordered phase above the transition temperature and non-zero during the transition to the ordered phase. The order parameter characterizes the breaking of symmetry occurring in phase transitions. According to the standard classification, phase transitions are of two types: the first kind, when the order parameter changes abruptly, and the second kind, when the order parameter changes continuously.

In recent years, interest in the study of new magnetic states of electron spins of substances has increased. In nanoelectronics, the local magnetic field created by the rotation of an electron around itself is used. The effect of an external magnetic field or a spin-polarized electric current can change the direction of the electron spin. Such a state of materials differs from classical ferromagnets, ferrimagnets and antiferromagnets in terms of their properties.

Copper chalcopyrite compounds are one of the most promising materials for research of spintronics. The extent of magnetic diversity of magnetic structures in chalcopyrites is mainly based on the structural properties of the Cu^{2+} ion. Other magnetoactive ions prefer certain types of crystallographic positions. For example, Fe^{3+} and Mn^{2+} ions mainly occupy octahedral, sometimes tetrahedral positions. Besides the octahedral and tetrahedral chalcogen surroundings, the Cu^{2+} ion can also have square and pyramidal surroundings. Such "properties" of the Cu^{2+} ion are explained by the features of its electronic structure, which allows it to adapt to different types of chalcogens.

TlBX_2 (B=Fe, Cr, Co, Ni, Ga, In; X=S, Se, Te) type triple semiconductor compounds have a layer-chain structure. They are characterized by anisotropic physical properties, which ensure the free movement of their charge carriers within the layers. This limits the

movement of carriers between layers as a result of van der Waals interactions and the fact that the wave functions of adjacent layers overlap less.

The object and subject of the research:

ABX₂: CuFeTe₂ (a, b, c), TlFeS₂, TlFeSe₂, TlCrS₂, TlCrSe₂, TlCoS₂, TlCoSe₂, TlNiS₂, TlNiSe₂ and solid solutions in (TlFeS₂)_{1-x}(TlGaS₂)_x, (TlFeSe₂)_{0.5}(TlGaSe₂)_{0.5}, (TlGaS₂)_{0.95}(TlCoS₂)_{0.05}, (TlInSe₂)_{1-x}(TlGaTe₂)_x type compounds, the temperature regions of phase transitions and their charge carrier transfer phenomena were revealed.

As a result, investigation of phase transitions (PT), electrical conduction mechanisms, and magnetic properties of low-dimensional semiconductors under various external conditions is a pressing issue. Researches were carried out in magnetic fields up to 50kOe and in the temperature range of 2÷400K.

The purpose and tasks of the research:

ABX₂ (A=Cu, Tl; B=Fe, Cr, Co, Ni, Ga, In; X=S, Se, Te) type of low-dimensional semiconductor chalcogenides and their solid solutions of phase transitions (magnetic, magnetoelectric and metal-dielectric type) consists of determining their compliance and determining the mechanisms of charge transfer and their prospective application as active materials in spintronics and semiconductor electronics.

For this purpose, the following tasks were set and solved in the work:

- Determination of structure symmetry and structure in Cu_{1.15}Fe_{1.23}Te₂ single crystal grown by gas transport method.
- Investigation of temperature dependences of conductivity below phase transition temperatures of CuFeTe₂, TlFeS₂ (Se₂) and TlFe_{0.975}Ga_{0.025}S₂ single crystals.
- Analysis of the transition temperature of the spin-glass state of the single crystal under the influence of the magnetic field on the chalcopyrite-type CuFeTe₂ single crystal.
- Analysis of the dependence of the mutual antiferromagnetic exchange between magnetic "clusters" in CuFeTe₂ single crystals on the arrangement of iron (Fe⁺³) cation and tellurium (Te⁻²) anion.
- Magnetic regularity of TlMeX₂ (Me=Fe, Cr, Ni and X=S, Se) compounds and their solid products with time-jump conductivity.

- Effect of changing their ratios ($x=0.025, 0.05, 0.075$ and 0.01) on the Neel temperature in $(\text{TlFeS}_2)_{1-x}(\text{TlGaS}_2)_x$ solid solutions.
- Study of the activation energies of TlCoS_2 and TlCoSe_2 ferrimagnets before and after the magnetic phase transition.
- Determination of the metal-dielectric phase transition in the hexagonal TlNiS_2 compound at the transition temperature. Investigation of the transition of this phase transition at the temperature of 240-245K.
- Investigation of the proportionality between alternating current conductivity and current frequency in the range of 3.2÷35 kHz of $(\text{TlInSe}_2)_{1-x}(\text{TlGaTe}_2)_x$ ($x=0.4$ and 0.6) solid solutions.

Research methods:

The quality and composition of the samples were controlled by following the production technology of the conducted studies, using XRDD2 PHASER x-ray device and EDX (Energy Dispersive X-ray Analysis), Analyst-800 Perkin Elmer type analyzers.

It was studied using the standard research methods of magnet (SQUID magnetometer, SQUID - Superconducting Quantum Interference Device) and kinetic properties applied for the study of semiconductor materials, as well as ПИУС-1УМ-К - device for determining the type of semiconductor materials. Experimental methods tested on relevant materials were used and results studied by other methods were cited. Magnetic properties of ABX_2 type ($\text{A}=\text{Cu}, \text{Tl}; \text{B}=\text{Fe}, \text{Cr}, \text{Co}, \text{Ni}, \text{Ga}, \text{In}; \text{X}=\text{S}, \text{Se}, \text{Te}$) low-dimensional semiconductors and their solid solutions studied in wide temperature ranges (2÷400K). electrical, thermoelectric and thermal properties were studied.

The main provisions submitted to the defense:

1. It is shown that $\text{Cu}_{1.15}\text{Fe}_{1.23}\text{Te}_2$ single crystal grown by gas transport has a tetragonal structure with structural symmetry $D_{2h}^2=P4/nmm$ and lattice constants $a=0.402\text{nm}$, $c=0.604\text{nm}$.

2. It was determined that in the chalcogen compounds CuFeTe_2 , TlFeS_2 , TlFeSe_2 and in their solid solution, a break in the temperature dependence of conductivity is observed below the phase transition temperature of $\text{TlFe}_{0.975}\text{Ga}_{0.025}\text{S}_2$ single crystals.

3. It was determined that in single crystals of chalcopyrite type CuFeTe_2 (a, b, c) there is an anomaly in temperature dependences of heat capacity and magnetic susceptibility $\chi(T)$ at Neel temperature and spin-glass state.

4. It was determined that the transition temperature of the spin-glass state decreases with increasing magnetic field in CuFeTe_2 single crystals.

5. It is shown that in single crystals of CuFeTe_2 , there is mutual antiferromagnetic exchange between magnetic "clusters". In this case, the iron (Fe^{+3}) cation is located between two tellurium (Te^{-2}) anions, and the magnetic moments of the spins are aligned opposite to each other parallel to the (001) plane. While CuFeTe_2 single crystals have $Z=1$ for their crystal structure, the magnetic crystal structure consists of eight formula units, i.e. $Z=8$.

6. It has been shown that the charge transport of TlMeX_2 ($\text{Me}=\text{Fe}$, Cr , Ni and $\text{X}=\text{S}$, Se) compounds and their solid products in the temperature ranges of magnetic order occurs with a jump.

7. It was shown that in $(\text{TlFeS}_2)_{1-x}(\text{TlGaS}_2)_x$ solid solutions, changing their ratios ($x=0.025$, 0.05 , 0.075 and 0.01) leads to a decrease in Neel temperatures and an increase in activation energies.

8. It was shown that the jump length of the specific electrical conductivity along the natural layers of the single crystal of $(\text{TlFeSe}_2)_{0.5}(\text{TlGaSe}_2)_{0.5}$ solid solution was $R_{\text{or.}}=23.3\text{nm}$. At the same time, a temperature hysteresis related to the proportional and non-proportional phases of the TlGaSe_2 single crystal is observed in the temperature dependence of the specific resistance.

9. It was determined that the activation energy of TlCoS_2 and TlCoSe_2 ferrimagnets was $\Delta E_a=0.009\text{eV}$, $\Delta E_a=0.005\text{eV}$ before the magnetic phase transition, and $\Delta E_a=0.116\text{eV}$, $\Delta E_a=0.014\text{eV}$ after the transition, respectively.

10. It is shown that a metal-dielectric phase transition occurs in the hexagonal TlNiS_2 compound at the transition temperature (240K). At temperatures above this phase transition, the conductivity changes from p-type semiconductor to metallic conductivity.

11. It was determined that dielectric loss in $(\text{TlInSe}_2)_{1-x}(\text{TlGaTe}_2)_x$ ($x=0.4$ and 0.6) solid solutions occurs due to direct conduction. In the

range of 3.2÷35 kHz, their alternating current conductivity is proportional to the 0.8 power of the frequency ($\sigma_{ac} \sim f^{0.8}$).

Scientific novelty of the study:

1. It was determined that a phase with symmetry $D_{2h}^2 - P4/nmm$ is formed in the $Cu_{1.15}Fe_{1.23}Te_2$ monocrystals grown by the gas transport method in the tetragonal structure. The X-ray study found that for $Cu_{1.15}Fe_{1.23}Te_2$, the main parameters of the crystal lattice, $a=0.402nm$, $c=0.604nm$ and the ratio of lattice parameters $c/a=1.5$, volume $v=0.09745nm^3$, densities $\rho_{calc}=6.764g/cm^3$ and $\rho_{prengen}=6.76g/cm^3$.

2. It has been shown that in single crystals of $CuFeTe_2$ type (a, b and c) below the semiconductor-metal phase transition temperature (PTT=125K) there is a deviation in the temperature dependence of the conductivity, which is explained by the change in activation energy. In that temperature range, the charge transport process occurs with a variable hopping length. The activation energy of the semiconductor-metal phase transition increases with an increase in the amount of iron in the compound.

3. In the temperature dependences of the magnetic susceptibility, $\chi_{H=0}^{ZFC}(T)$ and $\chi_{H=1kOe}^{FC}(T)$ broadening is observed, which is related to $CuFeTe_2$ (a, b and c) clustering. It was determined that in single crystals of $CuFeTe_2$ (a, b and c) a decrease in the transition temperature to the spin-glass state is observed with increasing magnetic field.

4. It was determined that the mutual magnetic exchange between magnetic "clusters" ($Cu^+-Te^{2-}-Fe^{3+}=Te^{2-}$) in $CuFeTe_2$ type compounds (a, b and c) is antiferromagnetic. At this time, Fe^{3+} cations are located between two Te^{2-} anions, and the magnetic moments of the spins are parallel to the (001) plane and opposite to each other. Effective magnetic moments of paramagnetic clusters are calculated for weak (100÷1000 Oe) and strong (10÷50 kOe) magnetic fields, paramagnetic Curie temperature (Θ_P) is

negative. It was determined that the magnetic crystal structure of CuFeTe_2 consists of eight formula units - $8(\text{CuFeTe}_2)$ $Z=8$, and the crystal structure is $Z=1$. Anisotropy parameter $\eta=0.309$, three-dimensional Debye temperature $\Theta_D=176.9\text{K}$ and two-dimensional Debye temperature $\Theta_2=122.2\text{K}$ of CuFeTe_2 type compound were found.

5. It is shown that in TlFeS_2 , TlFeSe_2 , TlCrS_2 samples, $(\text{TlFeS}_2)_{0.975}(\text{TlGaS}_2)_{0.025}$ and $(\text{TlGaSe}_2)_{0.5}(\text{TlFeSe}_2)_{0.5}$ solid solutions are determined by $\text{Mo}\pi\text{ttt}$ coordinates in the magnetically arranged temperature range $\lg\sigma=f(T^{-1/4})$ and has a variable length hopping conduction mechanism.

6. It was found that the increase of $x=0.025, 0.05, 0.075$ and 0.1 in the composition $(\text{TlFeS}_2)_{1-x}(\text{TlGaS}_2)_x$ leads to a decrease in the Neel temperature (T_N) and an increase in the activation energy, gallium and iron in this magnetic structure is explained by the redistribution of cations.

7. It was determined that the Neel temperature changes from 150K to 180K when samples of $(\text{TlFeS}_2)_{0.975}(\text{TlGaS}_2)_{0.025}$ solid solution are compressed under pressure $P=1.5 \times 10^3 \text{kg/cm}^2$.

8. The temperature dependence of the resistance of $(\text{TlGaSe}_2)_{0.5}(\text{TlFeSe}_2)_{0.5}$ solid solution shows a temperature hysteresis of $T_{\text{gis}}=109 \div 120\text{K}$, which is related to the commensurate and incommensurate phases of TlGaSe_2 single crystal.

9. It is shown that the activation energy values are calculated before and after the magnetic phase transition temperature in $\text{Tl}(\text{Fe, Cr, Co, Ni})\text{S}_2(\text{Se}_2)$ crystals and their solid solutions. The difference between these values (before and after PT) indicates the energy of the magnetic phase transition collapse.

10. It was determined that the TlNiS_2 compound has a jump conduction mechanism with a variable length ($R_L=3.0\text{nm}$)

localized near the Fermi level in a constant electric field. It was determined that the metal-dielectric (MD) phase transition in TlNiS_2 with hexagonal structure occurs at the Curie temperature $T_C=240\text{K}$ and at temperatures below T_C and is accompanied by a sharp jump of electrical resistance $(\rho/\rho_{\text{room}}) 10^3$. Thermo-EMF is greater than $S(T)$ by more than $10^2 (S/S_{\text{Room}})$. The temperature dependence $\rho(T)$ for TlNiSe_2 crystals during the MD phase transition is observed at $T_N=120\text{K}$, and at this temperature the inversion of the thermo-EMF $S(T)$ sign occurs.

11. It has been shown that the dielectric losses in samples of solid solutions $(\text{TlInSe}_2)_{1-x}(\text{TlGaTe}_2)_x$ ($x=0.4$ and 0.6) are related to conductivity. In the $f=3.2\div 35\text{kHz}$ frequency range, their variable conductivity (σ_{ac}) obeyed the regularity $\sigma_{\text{ac}}\sim f^{0.8}$, which is characteristic of the hopping mechanism of charge transfer through states localized near the Fermi level.

Theoretical and practical significance of the study:

The importance of the research conducted is determined by the fact that its results can be used to improve production and quality control methods. The results of the work can be used in the selection of electrical conductivity and magnetic properties, in the development of magnetic energy-independent memory. In addition, the research results facilitate the use of the studied materials in the devices of spin-dependent carriers of these or other charge carriers, including in magnetic tunnel structures. The optimal conditions for the synthesis of CuFeTe_2 single crystals were determined. A photo-accumulator can be created with the help of CuFeTe_2 bonding layer. These layers of CuFeTe_2 single crystals are used to measure the pressure of oxygen gas (O_2). Based on copper chalcogenides such as $\text{Al-Al}_2\text{O}_3\text{-CuFeTe}_2$ (Cu_{2-x}Te), it is possible to create multi-position converters in tunnel structures with Al_2O_3 thickness from 0.3 nm to 10 nm. $(\text{TlInSe}_2)_{1-x}(\text{TlGaTe}_2)_x$ (where $x=0.1, 0.2, 0.4$ and 0.6) solid solutions can be a base material for spintronics. The activation energies calculated before and after the magnetic phase transition of $\text{Tl}(\text{Fe}, \text{Cr}, \text{Co}, \text{Ni})\text{S}_2$ (Se_2) low-size single crystals can be used in theoretical calculations.

The obtained results have a prospective application as an active material in both spintronics and semiconductor electronics.

Approbation of work:

The main materials of the dissertation were presented and discussed at the following international conferences, meetings and seminars:

- Inorganic Materials Conference, Konstanz, Germany. 7-10 September 2002, Abs. Ref. Number 38.

- Abstracts of 13-th International Conference on ternary and multinary Compounds - ICTMC-13, Paris, France. Code Number 20 (SO3 A020), October 14 – 18, 2002, P.P. 2-1.

- International conference on Technical and Physical Problems in Power Engineering, Baku – Azerbaijan, № 93, 2002, p. 366-369.

- TPE – 06 3-rd International Conference on technical and Physical Problems in Power Engineering Turkey, Ankara., May 29-31, 2006, p. 607- 609.

- Сб. док.IV-ой Международной научной конференции «Актуальные проблемы физики твердого тела ФТТ-2009». Минск. Беларусь. 20 – 23 октября. 2009, т. 2, с.127-129.

- Bakı Dövlət universiteti. Fizikasının müasir problemləri V-ci respublika konfransı “Opto-, nanoelektronika və kondensə olunmuş mühit fizikası” material. Bakı 16-17 dekabr, 2011, s. 85-86.

- Fizikanın Müasir Problemləri. VI Respublika Konfransının Materialları “Opto, nanoelektronika, kondensə olunmuş mühit və yüksək enerjilər fizikası”. Bakı. Azərbaycan. 14 – 15 dekabr, 2012. s.163 – 165.

- Труды XVII-ой Международной конференции «Опто-наноэлектроника, нано технологии и микросхемы». Ульяновск, Россия. 15-19 сентября 2014, с. 79-80.

- Тезисы докладов Шестой Международной конференции «Кристаллофизика и деформационное поведение перспективных материалов», посвященной 90-летию со дня рождения проф. Ю.А. Скакова. Москва. 26-28 мая 2015, с. 223.

- Nineteenth Symposium on Thermophysical Properties, University of Colorado at Boulder, CO, USA. June 21-26, 2015, pp. 272.

- Труды международной конференции: «Фундаментальные и прикладные вопросы физики», 13-14 июня Ташкент, т. 2, 2017, с. 44-46.

- Восьмая Международная конференция «Кристаллофизика и деформационное поведение перспективных материалов» 5–8 ноября 2019 Москва, с. 162.

Publications:

36 scientific articles(12 of them in journals with international citation indexes - ICI) have been published on the topic of the dissertation: 25 articles in publications recommended by the SAC under the President of the Republic of Azerbaijan and 11 conference materials.

Participation of author:

The topic, idea and main direction of research of the dissertation work are defined by the author. The main goal and the issues that need to be solved during the research were evaluated by the author. ABX_2 (A=Cu, Tl; B=Fe, Cr, Co, Ni, Ga, In; X=S, Se, Te) and their basic solutions, processing of results and their analysis, general provisions for defence, conclusions and recommendations compiled.

Name of the organization where the work is done:

The dissertation work was carried out in the "Resonance Phenomena in Solids" laboratory of the Physics Institute of the Azerbaijan National Academy of Sciences.

The scope, structure and main content of the dissertation:

The submitted dissertation consists of an introduction, six chapters, main conclusions and a bibliography of 203 names. The work of the dissertation consists of a total of 381,754 signs, 82 pictures and 13 tables.

The content of the work

The introduction substantiates the relevance of the chosen research topic, formulates the purpose and main tasks of the dissertation work, scientific novelty, practical significance of the work, presents the main scientific provisions submitted for defense,

and briefly outlines the main content of individual chapters of the dissertation work.

The first chapter is devoted to the review of research studies of phase transition and jump conductance of low-dimensional crystals.

This chapter discusses the fluctuation magnetic structures that arise in magnetic systems of low-dimensional crystals with antiferromagnetic exchange and interactions. Due to strong quantum fluctuations in the competition of exchange interactions between the nearest ions and second neighbors in the chain, such systems exhibit a wide range of unusual magnetic structures.

One of the most promising classes for spintronics research and study is copper chalcogen compounds or chalcopyrites.

In a number of semiconductor compounds with the general formula ABX_2 , the metal atoms A and B tend to exhibit different valences, which allows obtaining new materials for spintronics and semiconductor optoelectronics.

Compared to other groups of substances, 3d compounds have a surprisingly wide variety of electrical properties. Triple $TiMeX_2$ (Me=Fe, Cr, Co, Ni and X=S and Se) compounds belong to the class of anisotropic magnetic semiconductors.

Electronic structures, electrical and magnetic properties in chalcogenides of transition metals are complicated by the presence of 3d-electrons. These properties can best be analyzed by extending the molecular-orbitals and band model to include d-electrons.

The metal-dielectric Transition (MDT) belongs to the class of electronic phase transitions, because its main characteristic is the reconstruction of the electronic energy spectrum - the generation of a spin density wave (SDW) and a charge density wave (CDW) energy band that separates the under-occupied states and the over-unoccupied states. In most cases, the temperature dependence of the electrical resistivity $\rho(T)$ changes abruptly at the Curie temperature T_C point, which indicates a phase transition of the first type. Sometimes this case is small or non-existent, so it is possible to have a first-type phase transition or a second-type phase transition close to a second-type phase transition.

In the last few years, structural phase transitions in layered thallium compounds of type $TlBX_2$ (where $B=In^{3+}$, Ga^{3+} and $X=S$, Se , Te) have been discovered and are intensively studied. In all these layered crystals, below a certain temperature T_0 , displacement of atoms occurs from the equilibrium state of the extreme structure - the basic lattice. The period of this extreme structure is, as a rule, not proportional to the period of the main lattice (lattice above T_0), and with the subsequent decrease in temperature, the extreme structure approaches a structure proportional to the initial structure, either continuously or abruptly.

Studying the lattice dynamics of such materials provides information that reflects and characterizes the nature of changes in intra- and interlayer interactions, on the basis of which various microscopic models can be constructed.

The second chapter is devoted to structural-crystalline chemical properties of chalcopyrite and $CuFeTe_2$ kind compounds of its various types. In this chapter, all the known facts are summarized and a large group of tetrahedral coordination semiconductor compounds is considered based on the principle of close approach. After looking at the crystal-chemical properties of this class of compounds, the reasons for the formation of phases in chalcopyrite and its different types of structures and their compliance with the law are explained. The main physical-chemical properties of triple and more complex compounds are analyzed and appropriate conclusions are drawn about the differences and contradictions obtained from the experimental results of various authors.

X-ray structure studies showed that plate-like crystals are tetragonal: $a=0.402$ nm, $c=0.604$ nm, space group $P4/nmm$, $Z=1$, $\rho=6.5g/cm^3$. X-ray structure studies also showed that chalcopyrite-type $CuFeTe_2$ (a, b, c) single crystals are the most perfect.

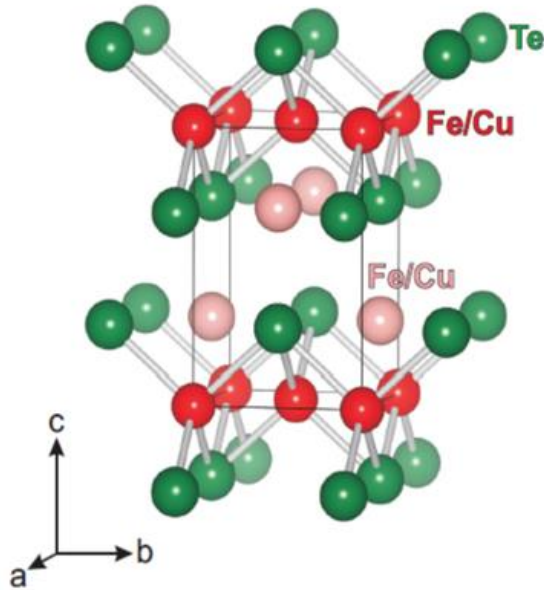


Image. 1. Crystal structure of CuFeTe_2

Figure 1. shows the crystal structure of CuFeTe_2 , where the Cu and Fe atoms (marked in red) are located in $2a(0\ 0\ 0)$ crystallographic positions with about 50% for each of these atoms. Te atoms (marked in green) are located in $2c(0\frac{1}{2}z)$ crystallographic positions. Additional sites in $[2c'-(0\frac{1}{2}z')]$ crystallographic positions (marked in pink) are partially filled with Cu and Fe atoms, less than 15% capacity. Therefore, in order to determine the nominal composition of single crystals and clarify their crystal structures, they were analyzed in an EDX-type analyzer (Energy Dispersive X-ray Analysis) in an x-ray device and repeated by the analysis method in a Perkin Elmer Analyst-800 device.

The automatically calculated atomic percentages correspond to the following values:

- for single crystals of CuFeTe_2 grown from stoichiometric composition: $\text{Cu}=24.53 \pm 1.85$; $\text{Fe}=28.68 \pm 1.86$; $\text{Te}=46.79 \pm 2.27$;
- for $\text{Cu}_{1.15}\text{Fe}_{1.23}\text{Te}_2$ single crystals grown from polycrystalline composition: $\text{Cu}=27.95 \pm 1.98$; $\text{Fe}=25.47 \pm 1.61$; $\text{Te}=46.59 \pm 2.18$ (in

atomic percent for composition). The chemical composition of single crystals calculated on the basis of the above analysis values corresponds to the formula $\text{Cu}_{1.15}\text{Fe}_{1.23}\text{Te}_2$.

The structural formula of chalcopyrite type single crystals is as follows:

$\text{Cu}^{1+}\text{Fe}^{3+}\text{Te}_2$ ($\text{Cu}_{0.22}$ and $\text{Fe}_{0.1}$), $\text{Cu}^{1+}\text{Fe}^{3+}\text{Te}_2$ ($\text{Cu}_{0.13}$ and $\text{Fe}_{0.22}$) and $\text{Cu}^{1+}\text{Fe}^{3+}\text{Te}_2$ ($\text{Cu}_{0.15}$ and $\text{Fe}_{0.23}$) and "excess" Cu (metal atoms (one- or two-valent) and Fe (two- or three-valent) are chaotically located in the cavities of the crystal lattice and behave as additives (nanoparticles).

In normal group metals, the exchange forces in the system of collective electrons are broken by the Fermi energy and cannot lead to the formation of magnetic order. The situation may be more favorable for exchange forces in compounds of transition 3d-metals. Considering that the crystal structure of a solid body has 230 spatial symmetry groups, and the atomically ordered magnetic structure has 1651 spatial symmetry groups, therefore, in some cases, ferromagnetism or antiferromagnetism is observed in them as a result of the dominance of exchange relationships. By maintaining a significant localization of charge and spin density in the crystal nodes, the existence of narrow energy bands of the former internal 3d-electrons makes possible the spin regularization of the collected s- and d-electrons in the 3d-system of metals and compounds. Thus, the origin of the exchange bond of electronic magnetic moments in semimetals and semiconductors is due to the active influence of conduction electrons on the system of uncompensated magnetic moments of former 3d-electrons.

In crystals which have antiferromagnetic order, when conduction electrons move from one magnetic sublattice node to another sublattice node, electron spin moves from one node with a certain value and direction to another node with a different spin value and direction. Therefore, the state of conduction electrons in a crystal with several magnetic sublattices must differ significantly from the state of conduction electrons in a crystal with one sublattice or in a paramagnetic crystal. The difference is that in an antiferromagnetic crystal, spatial degeneration of conducting electrons is partially removed, because the presence of several magnetic sublattices causes a change in the

periodicity of the potential field in which the electrons move (that is, a decrease in its symmetry). In this case, for conduction electrons with different projected spins, the shift of energy subbands does not occur, but nevertheless the energy spectrum can change significantly. For example, in the middle part of the 4s-energy band of conduction electrons, it is possible to create a forbidden part ΔE_{af} , similar to what happens in alloys during atomic ordering.

Thus, the presence of magnetic order in the transition metal crystal leads to significant changes in the energy spectrum of conduction electrons. Moreover, two main effects are observed here:

- 1) elimination of spin degeneration (by direction) and
- 2) elimination of space degeneration.

The results of the conducted experimental studies answer all the questions of the existing disagreements in these materials and allow us to draw new conclusions about the process of phase formation and the manifestation of these or other properties. In this chapter, enough space is also given to the chemical analysis of single crystals grown from different compositions of polycrystals.

Then, the results of studies of electrical conductivity (σ), thermo-EMF(S), magnetic susceptibility(χ), magnetization(M) of CuFeTe₂(a, b and c) type chalcopyrite single crystals in a wide temperature range are explained.

The investigated low-dimensional ABX₂ (A=Cu, Tl; B=Fe, Cr, Co, Ni, Ga, In; X=S, Se, Te) type semiconductors and their solid solutions were pressed under a pressure of $P=1.5 \times 10^3 \text{ kg/cm}^2$ and have the shape of a rectangular parallelepiped designed for electrical measurements. Before striking the contacts, they are heated to a temperature of $\sim 450\text{K}$. Ohmic contacts are created by electrolytic deposition of copper. The electrical conductivity $\sigma(T)$ and thermo-EMF(S) coefficients of the obtained samples were measured with four probe methods up to 3% accuracy in the temperature range of $77\div 400\text{K}$.

Two main directions can be distinguished in the problem of phase transitions. First, it is related to the study of the behavior of the system properties around the critical temperature. Another direction on which the microscopic theory of phase transition is based is to analyze the

properties of the ground state of the system within the framework of one or another model concepts and explain the possible causes of its instability, under the influence of which the system changes to a newer, more favorable energy state. The process of merging these two directions into a single phase transition theory is currently being investigated.

The temperature dependences of the magnetic susceptibility $\chi(T)$ and the thermal capacity $C_p(T)$ repeat the dependence of $\chi(T)$, the presence of anomalies in the Neel temperature region, the generation and dissipation of spin-glass waves (SGW), and the locking temperature, repeating the dependence of $\chi(T)$ (characterized by T_L). For CuFeTe_2 (a, b, c) chalcopyrite-type single crystals, the Neel temperature $T_N=65\text{K}$ and the locking characteristic of supermagnets $T_B>360\text{K}$ were determined. Fe^{3+} cations are located between two Te^{2-} anions, and the antiferromagnetic magnetic moments of the spins are directed parallel to the opposite (001) plane. The magnetic crystal structure of CuFeTe_2 consists of eight formula units-8(CuFeTe_2) $Z=8$, whereas in the crystal structure it is $Z=1$. Effective magnetic moments of paramagnetic clusters were measured in weak (100÷1000Oe) and strong (10÷50kOe) magnetic fields and it was shown that weak $\mu_{\text{eff.}}\geq 0.7\mu_B$ and strong $\mu_{\text{eff.}}\sim 2.4\mu_B$ (μ_B is Bohr magneton). Below $T_g=55\text{K}$, the spin-glass state is observed in CuFeTe_2 (a, b, c) chalcopyrite type single crystals. The different behavior of the dependences of the $\chi^{\text{ZFC}}(T)$ magnetic field at zero and $\chi^{\text{FC}}(T)$ magnetic field at 1kOe during cooling below the locking temperature is one of the main signs indicating the clustering of the chalcopyrite-type CuFeTe_2 single crystal (Fig. 2).

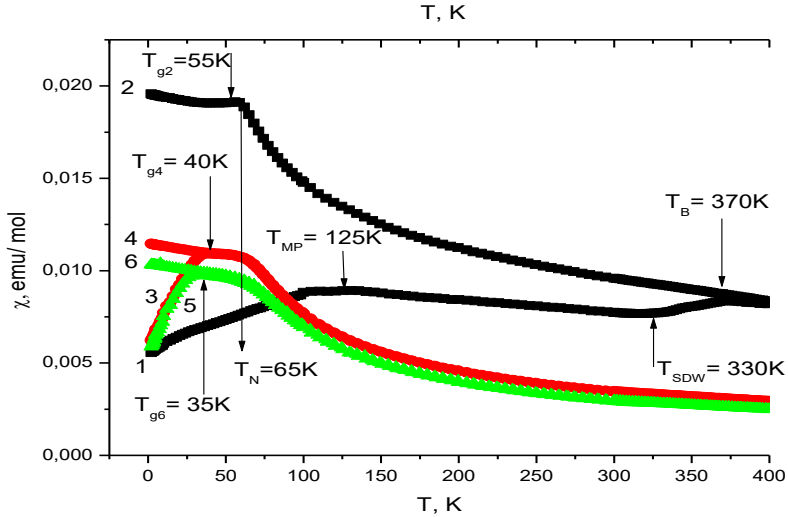


Fig. 2. Temperature dependence of magnetic susceptibility of $\text{Cu}_{1.13}\text{Fe}_{1.22}\text{Te}_2$ single crystal:

1-1.0, 3-10 and 5-20kOe in ZFC and FC – 2 – 1.0, 4 - 10 and 6 - 20kOe. Temperatures: $T_{MP}=125\text{K}$, spin-glass case in magnetic fields:

1.0 kOe – $T_{g2}=55\text{K}$, 10kOe – $T_{g4}=40\text{K}$ and 20kOe – $T_{g6}=35\text{K}$.

Spin density wave $T_{SDW}=330\text{K}$ and locking temperature $T_L=370\text{K}$

Effective magnetic moment $\mu_{\text{eff}}=2.0\div 2.4\mu_B$.

Fig. 2 shows the field dependence of magnetization (hysteresis) of chalcopyrite-type CuFeTe_2 single crystal at different temperatures. It is clear that at high temperatures (above 100 K), the magnetization (with field) increases almost linearly, as is characteristic of the paramagnetic region. At low temperatures (2K and 4K), a hysteresis loop is observed, which changes its position in the field dependence of magnetization (measurements were made in FC – 50÷0÷50kOe and the opposite mode). The hysteresis loop is wider and ferrimagnetic type. In all chalcopyrite-type CuFeTe_2 (a, b and c) single crystals, iron (Fe^{3+}) is also in the trivalent state, which agrees with Messbauer effect. It has been shown in the literature that the Messbauer spectrum of CuFeTe_2 consists of a single peak that splits into six components

due to the extremely weak magnetic interaction. This is due to the magnetically ordered atoms of iron (Fe^{3+}) occupying a position in the structure. The isomer shift is small, and the quadrupole splitting is absent. The observed parameters are consistent with the idea that magnetically bonded Fe^{3+} atoms are located in tetrahedral positions in high spin states. The residual magnetization was determined from the field dependence of the $M(H)$ magnetization (hysteresis) at different temperatures of CuFeTe_2 single crystal. It can be seen that at high temperature (above 100 K) the magnetization (with field) increases almost linearly, as is characteristic of the paramagnetic region. At low temperatures (2K and 4K), a shifted hysteresis loop is observed in the dependence of the magnetization on the field (measurements were made in the mode of the magnetic field $-50-0+50$ kOe). The hysteresis loop is wider and ferrimagnetic type. In all single crystals of CuFeTe_2 (a, b and c) type chalcopyrite, iron (Fe^{3+}) is in the trivalent state according to Mössbauer effect. It is shown in the literature that the Mössbauer spectra of CuFeTe_2 consist of a single peak divided into six components due to the extremely weak magnetic interaction. It is due to the magnetically arranged iron atoms (Fe^{3+}) occupying one position in the structure. The isomeric shift is small and there is no quadrupolar splitting. The observed parameters are consistent with the concept of magnetically bound Fe^{3+} atoms in a high spin state in tetrahedral positions.

Interatomic interaction in layered crystals leads to unusual temperature dependence of heat capacity with special laws at low temperatures. The same has been observed in anisotropic layered magnets where the phase transitions are variable in nature.

The heat capacity of $\text{Cu}_{1.04}\text{Fe}_{1.12}\text{Te}_{1.84}$ was measured on a commercial Quantum Design PPMS (Physical Property Measurement System) in the range 2-306K. Fig.3 shows the temperature dependence of the heat capacity (C_p), showing the experimental results, and the difference between the experimental heat capacity and the lattice heat capacity calculated according to the Debye model. $C_{p\text{exp}} - C_{pD} = \Delta C_p(T)$, where $C_{p\text{exp}}$ is the difference between experimental results and C_{pD} values of the lattice heat capacity calculated according to the Debye model. (The Debye temperature is

the temperature at which all frequencies of the given CuFeTe_2 compound are excited. Further increase in temperature does not lead to the creation of new oscillations, but causes an increase in the amplitudes of the existing ones, that is, the average energy of the oscillations increases with the increase in temperature.

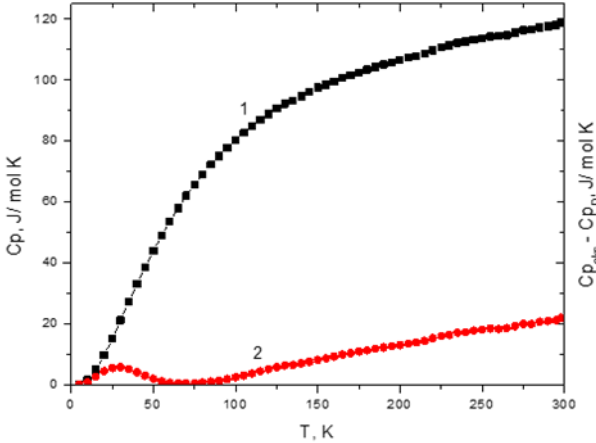


Fig.3. Temperature Dependencies of heat capacity.

Fig.3 shows the temperature dependence of heat capacity (1) and (2) additional heat capacity of $\text{Cu}_{1.04}\text{Fe}_{1.12}\text{Te}_{1.84}$ compound ($C_{\text{pexp}} - C_{\text{pD}}$). C_{p} and C_{pexp} are experimental value of heat capacity and C_{pD} are calculated lattice values of heat capacity according to Debye model. The $C_{\text{p}}(T)$ linear section covers the temperature range of 65-125K. The $\Delta C_{\text{p}}(T)$ curve (1) undergoes discontinuity at antiferromagnetic temperature $T_{\text{N}}=65\text{K}$ and spin-glass transformation.

Fig.3 clearly shows the phase transitions $\Delta C_{\text{p}}=0$ from the dependence of $\Delta C_{\text{p}}(T)$ antiferromagnetic-paramagnetic ($T_{\text{N}}=65\text{K}$) and spin-glass state ($T_{\text{g}}=55\text{K}$).

To see these phase transitions, the temperature dependence of the heat capacity versus temperature is shown in figure 4(a).

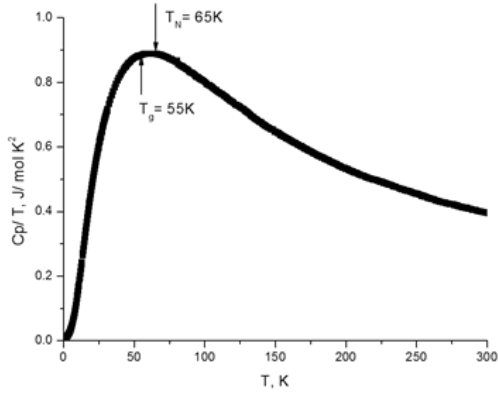


Fig.4. Temperature dependence of the ratio of heat capacity to temperature.

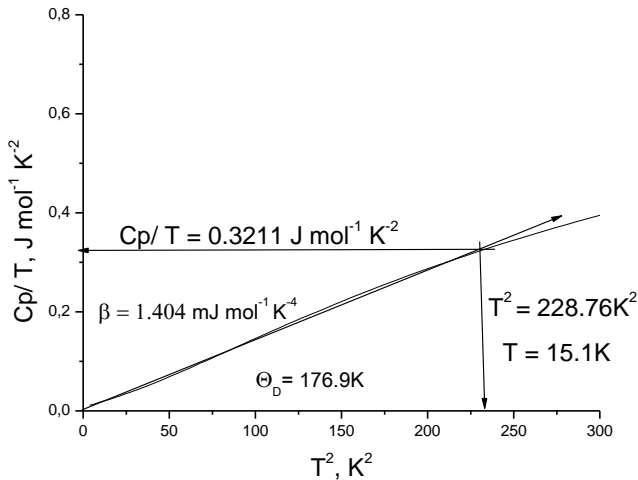


Fig. 4a. Dependence of the ratio of heat capacity to temperature on the square of temperature (Debye's cubic law).

In the temperature dependence of the heat capacity $\Delta C_p(T)$ it is spread close to the phase transition temperature and it determines the identity between the second type of phase transitions and critical

phenomena. Near the magnetic phase transition temperature, due to the development of fluctuations, the homogeneous phase is separated into a large number of spin "groups" that form a magnetically dispersed system. The temperature change at the phase transition reduces the dispersion and the system becomes homogeneous. The presence of this dispersion in the phase transition region leads to scattering of the maximum in the temperature curve of the heat capacity. The analysis of the results obtained at low temperatures clearly shows this. At low temperatures, the kinetic energy is small, so the behavior of the $C_p(T)$ and C_p/T dependences will be completely different. In the low kinetic energy region, the temperature dependence of C_p/T was established (Fig.4) and phase transitions due to small changes in potential energy in the curve were visible. Taking into account the unusual nature of the magnetic phase transition in $\text{Cu}_{1.04}\text{Fe}_{1.12}\text{Te}_{1.84}$, the temperature dependence of C_p/T , $C_{p\text{exp}}(T)$ is established on the basis of experimental data.

Fig.4 and 4a clearly demonstrate the unusual (diffusion, scattering and fluctuation) nature of the phase transition.

The results of experimental data processing according to the method described in this work are presented in fig.4a, where $n_0=4$ is the number of atoms in the molecule of the studied crystal, $3k_B N=R_g$ is the gas constant, N is Avogadro's number, k_B is Boltzmann's constant, Θ_D is the Debye temperature. The figure (Fig. 4a) shows the dependence of C_p/T on T^2 (Debye's cubic law). Within $T \ll \theta_D$

$$C_{\text{lattice}} \rightarrow \beta \cdot T^3 = 12 R \pi^4 / 5 \cdot (T/\theta_D)^3 \quad (1)$$

Debye temperature from experimental data:

$$\Theta_D = (1942.7 n_0 / \beta)^{1/3} \quad (2)$$

where $n_0=4$ is the number of atoms in the molecule of the studied crystal, calculated by the formula $\beta=1.452\text{mJ}\cdot\text{mol}^{-1}\text{K}^{-4}$. $\Theta_D=176.9\text{K}$ is the Debye temperature at $T \rightarrow 0\text{K}$. This indicates that the structural anisotropy in the compounds does not affect the heat capacity behavior below 15.1 K (Fig. 4a).

We used the characteristic equation for layered crystals with a linear part of the temperature dependence to determine the anisotropy parameter (η) and the two-dimensional Debye temperature (Θ_2). From Fig.4b, it is easy to evaluate $\eta=0.309$ and $\Theta_2=122.2\text{K}$ $C_p/3n_0k_B N=$

0.447 at $T=0$ and $\eta=0.309$, and $\Theta_2=(1 - \eta)\cdot\theta_D=122.2\text{K}$ where $\eta=|\Delta C_p/(1+\Delta C_p)|$.

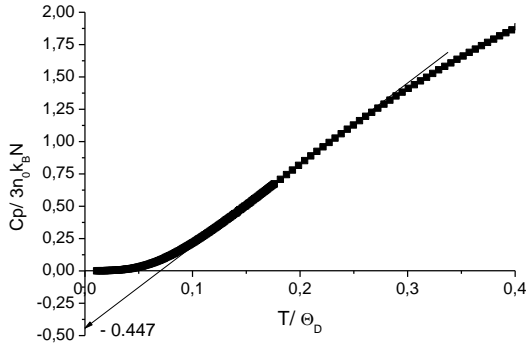


Fig.4b. Temperature dependence of heat capacity in $C_p/3n_0k_B N - T/\Theta_D$ coordinates.

The following conclusions are drawn from the above:

1. $\text{Cu}_{1.22}\text{Fe}_{1.10}\text{Te}_2$ (a), $\text{Cu}_{1.04}\text{Fe}_{1.12}\text{Te}_{1.84} \approx \text{Cu}_{1.13}\text{Fe}_{1.22}\text{Te}_2$ (b) and $\text{Cu}_{1.15}\text{Fe}_{1.23}\text{Te}_2$ (c) single crystals with $P4/nmm$ tetragonal structure were grown.

2. Superparamagnetic locking temperatures $T_L=358\text{K}$ (a), $T_L=360\text{K}$ (b) and $T_L=370\text{K}$ (c) and Neel temperature $T_N=65\text{K}$ were determined for single crystals of CuFeTe_2 (a, b and c). Magnetic moments parallel and perpendicular to the (001) plane and paramagnetic Curie temperature were calculated for CuFeTe_2 (a, b and c) type chalcopyrite AFM single crystals:

a) $\mu_{\text{eff}} \leq 0.7\mu_B$ in a magnetic field of $100 \div 1000\text{Oe}$ for CuFeTe_2 (a, b and c);

b) For CuFeTe_2 (a, b and c) $\mu_{\text{eff}} \parallel \approx 2.0 \div 2.6$ and $\mu_{\text{eff}} \perp = 2.0 \div 2.30\mu_B$ in $10 \div 50\text{kOe}$ magnetic field, as well as paramagnetic Curie temperature $\Theta_P \parallel$ and $\Theta_P \perp$ is negative.

It was determined that iron (Fe^{3+}) is trivalent in all CuFeTe_2 single crystals (a, b and c).

3. It is shown that CuFeTe_2 single crystals (a, b and c) exhibit a spin-glass state at freezing temperatures $T_g=35, 50$ and 55K , respectively.

4. It was determined that Fe^{3+} cations are located between two Te^{2-} anions, and the magnetic moments of the spins are directed parallel to the (001) plane, which is opposite to each other (antiferromagnetic). The magnetic structure of these crystals: $\text{Cu}^+-\text{Te}^{2-}-\text{Fe}^{3+}-\text{Te}^{2-}$ consists of four "clusters" located opposite each other.

5. It was established that the temperature dependences of electrical conductivity $\sigma(T)$ and thermo-EMF $S(T)$ of CuFeTe_2 (b) single crystal can be divided into four regions:

a) temperature range $77\div 121\text{K}$, semiconductor region: $\Delta E_a=0.008\text{eV}$ (a), $\Delta E_a=0.002\text{eV}$ (b) and $\Delta E_a=0.002\text{eV}$ (c);

b) temperature range $155\div 267.5\text{K}$ - where spin wave density (SDS) exists (metal domain): $\Delta E_a=0.013\text{eV}$ (a), $\Delta E_a=0.008\text{eV}$ (b) and $\Delta E_a=0.013\text{eV}$ (c), where (a), (b) and (c) are the activation energies of compressed single crystals;

The difference between the activation energies before and after the semiconductor-metal transition is the energy spent on the dissolution of this phase transition. This difference shows values of 0.005eV , 0.006eV and 0.011eV for chalcopyrite-type CuFeTe_2 (a, b and c), respectively. This is the energy spent on the breakdown of the semiconductor-metal phase transition, and the duration of this transition increases with the increase of iron ions.

c) temperature range of $289\div 360\text{K}$ - SDW is observed here;

d) $360\div 390\text{K}$ temperature range (after T_L locking temperature) – being in superparamagnetic state.

6. Anomaly in the metal-semiconductor (bivalent copper and iron) transition temperature region, degeneration and disintegration of SDW from the thermo-EMF $S(T)$ temperature dependence of the compound CuFeTe_2 (b), as well as the temperature dependence of the magnetic susceptibility $\chi(T)$ by reproducing T_L The locking temperature of is determined.

7. CuFeTe_2 at temperature $77\div 120\text{K}$ corresponds to a hopping charge transport mechanism with variable hopping length $R_L=2.1\text{nm}$ at 77K and $R_L=2.3\text{nm}$ at 120K . The density of localized states near

the Fermi level was determined in CuFeTe_2 $N_F=5.3 \times 10^{21} \text{eV}^{-1} \text{cm}^{-3}$. The average hopping distance calculated in CuFeTe_2 was $R_{av}=2.2\text{nm}$, and the energy spread of localized states near the Fermi level was $\Delta E=0.01\text{eV}$. The value of ΔE corresponds approximately to the average value of the activation energy of the hopping in CuFeTe_2 , which is $\Delta W=0.005\text{eV}$. The approximate concentration of localized states in the CuFeTe_2 band gap was $N_t=5.3 \times 10^{19} \text{cm}^{-3}$.

8. Experimental studies have shown that magnetic interactions ($\text{Cu}^+-\text{Te}^{2-}-\text{Fe}^{3+}-\text{Te}^{2-}$) are antiferromagnetic "clusters". It should be noted that the magnetic structure of these chalcopyrite single crystals of type CuFeTe_2 (a, b and c) consists of eight formula units - $8(\text{CuFeTe}_2)$ $Z=8$, so $Z=1$ in the crystal structure. Fe^{3+} cations are located between two Te^{2-} anions, and their magnetic spins are directed parallel to each other (antiferromagnetically) parallel to the (001) plane.

9. In this case, one of the two Te^{2-} 3p valence electrons can be transferred to the half-filled layer of the Fe^{3+} transition metal ion (with five 3d electrons), and according to Hund's rule, its spin will be antiparallel to the spin of five d-electrons. The spin of the second remaining electron in tellurium ions will be antiparallel to the spin of the first electron (according to the Pauli exclusion principle). The same relationship with the antiparallel arrangement of unpaired electrons can occur with another metal ion (Fe^{3+}) on the opposite side of the tellurium ion.

10. The detected spin-glass ($T_g=55\text{K}$) and antiferromagnetic ($T_N=65\text{K}$) phase transitions are characterized by the deviation of the heat capacity in the dependence of C_p/T on T , characteristic of quasi-two-dimensional materials.

11. Anisotropy parameter $\eta=0.309$. The three-dimensional (3D) Debye temperature $\Theta_D=176.9\text{K}$ and the two-dimensional (2D) Debye temperature $\Theta_2=122.2\text{K}$ are found.

TlFeX_2 triple compounds are 3d-compounds compared to other groups of matter and have extremely different electrical properties. TlFeX_2 triple compounds belong to the class of anisotropic magnetic semiconductors. Single crystals of TlFeS_2 and TeFeSe_2 were grown by the modified Brigman-Stockbarger method. The conducted

structural studies showed that the received TlFeS_2 crystals have a chain structure and the parameters of the crystal lattice take the following values: $a=1.1643$, $b=0.5306$, $c=0.6802\text{nm}$; $\beta=116.75^\circ$, space group $C2/m$. TlFeSe_2 unit cell parameters $a=1.202$, $b=0.55$, $c=0.713\text{nm}$; A monocline with $\beta=118.52^\circ$ crystallizes in syngony.

The samples for electrical measurements were pressed into TlFeS_2 and TlFeSe_2 crystal fibers under pressure and took the shape of a parallelepiped with dimensions of $12.5 \times 5.0 \times 1.3\text{mm}^3$ and $12.5 \times 5.0 \times 2.3\text{mm}^3$, respectively. Pressed ($P=10^3\text{kg/cm}^2$) samples were then annealed at 450K . Ohmic contacts are created by electrolytic deposition of copper. Electrical conductivity (σ) and thermo-EMF coefficients (S) of TlFeS_2 and TlFeSe_2 samples were measured by four probe methods in the temperature range of $85 \div 400\text{K}$ [78, 154, 166] .

At the Neel temperature, a small deviation of the conductivity from the temperature dependence of the electrical conductivity $\sigma(T)$ is observed, which is explained by the change in the activation energy of the hopping process. It is clear from the experimental results that the conductivity of the TlFeS_2 sample at $T < 200\text{K}$ and for the TlFeSe_2 sample above 250K does not depend on the temperatures. The temperature-independent conductivity can be related to the collapse of the antiferromagnetic order of these crystals ($T_N=196\text{K}$ and 290K , respectively)³.

From the thermo-EMF $S(T)$ temperature dependence of TlFeS_2 compound, there is an inversion of sign at Neel temperature $T_N=196\text{K}$, and for TlFeSe_2 at 290K . The effect on the formation of the Sp-d interaction consists in the change of the sign of the temperature dependence of the thermo-EMF and the appearance of a negative $S(T)$ section at high temperatures. A further increase in temperature leads to the depletion of this previously completely filled subzone. The latter leads to an increase in the number of current carriers through holes in a given d -subsystem. At the same time, carriers in the other d -subsystem, whose energies shift down, also increase. Magnetic studies of TlFeS_2 and TlFeSe_2 compounds show an antiferromagnetic phase transition below $T_N=196\text{K}$ for TlFeS_2 single crystals and $T_N=290\text{K}$ for TlFeSe_2 . Magnetic susceptibility measurements for

single crystals of TlFeS_2 and TlFeSe_2 in the temperature range of $2\div 400\text{K}$ showed the behavior characteristic of quasi-one-dimensional antiferromagnets. These magnetic studies are consistent with neutron diffraction and EPR measurements. $(\text{TlFeS}_2)_{0.975}(\text{TlGaS}_2)_{0.025}$ solid solution study of temperature dependence of conductivity and thermo-EMF coefficient is shown in fig.5.

For electrical measurements, $(\text{TlFeS}_2)_{0.975}(\text{TlGaS}_2)_{0.025}$ samples have a parallelepiped shape: 1 - single crystal $14.48\times 1.4\times 1.26\text{mm}^3$ and 2 - pressed single crystal $10.9\times 5.27\times 1.0\text{mm}^3$, 3 - rubbed and pressed $8.7\times 5.09\times 1.14\text{mm}^3$.

Contacts to the head and foot planes with the crystals are created by electrolytic deposition of copper. The temperature dependences of electrical conductivity (σ) and thermo-EMF (S) of the obtained samples were measured with an accuracy of up to 3% by the four-probe method in the temperature range of $80\div 355\text{K}$. The amplitude of the external constant electric field applied to the studied samples during electrical measurements corresponds to the ohmic region of VA [1, 60, 85, 87]. Experience shows that at low concentrations (up to 10%) of substitutional cations, the resistance of solid solutions usually increases. This may indicate that at low concentrations the substituted cations cannot be evenly distributed in the crystals, resulting in local violations of the crystal symmetry. This can lead to a decrease in the free path of electrons and, accordingly, their mobility.

With the increase in the concentration of the substituted gallium cation (x) in solid solutions, the mechanism of interaction between the dopant centers, expressed in practice by conductivity, is activated. As the temperature rises, the internal conduction mechanism gradually begins to take effect, and the dependence $\ln\sigma=f(T)$ becomes exponential.

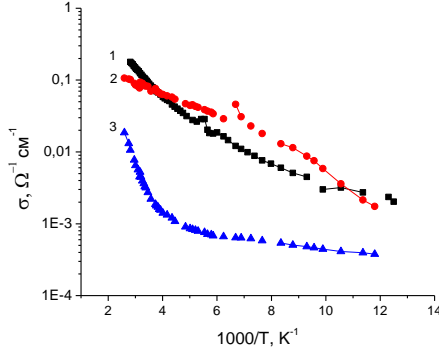


Fig. 5. $(\text{TlFeS}_2)_{0.975}(\text{TlGaS}_2)_{0.025}$ sample $\sigma(1000/T)$ of electrical conductivity from temperature dependencies; 1 - single crystal (σ_{mon}), 2 – along the a axis pressed single crystal (σ_{p}) and 3 –rubbed and pressed. ($\sigma_{\text{ovul.p}}$).

It was calculated from Fig. 5 that the activation energy (ΔE_a) of $\text{TlFe}_{0.975}\text{Ga}_{0.025}\text{S}_2$ samples in the paramagnetic region in the temperature range above the Neel temperature: 1 - single crystal $\Delta E_{\text{amon}}=0.083\text{eV}$, 2 - pressed $\Delta E_{\text{ap}}=0.103\text{eV}$ - $\Delta E_{\text{aovul.p}}=0.337\text{eV}$.

In the magnetic ordered region at a temperature lower than T_N , the activation energy was: 1 – $\Delta E_{\text{amon}}=0.137\text{eV}$ for single crystal, 2 – $\Delta E_{\text{ap}}=0.063\text{eV}$ for pressed single crystal and 3 – $\Delta E_{\text{arub.p}}=0.02\text{eV}$ for rubbed and pressed single crystal. The differences of these activation energies were 1 – 0.054, 2 – 0.04 and 3 – 0.317eV, respectively, which was spent on energy dissipation in the AFM phase transition.

Fig. 6 shows the temperature dependence of thermo-EMF $S(T)$ of $\text{TlFe}_{0.975}\text{Ga}_{0.025}\text{S}_2$ solid solution.

1 - single crystal S_{mon} , 2 - pressed S_{p} and 3 - rubbed and pressed $S_{\text{rub.p}}$, get different values at Neel temperature (T_N). Thermo-EMF at the temperature of the magnetic phase transition of the $\text{TlFe}_{0.975}\text{Ga}_{0.025}\text{S}_2$ solid solution at the Neel temperature takes the following values:

- 1 – single crystal $S_{\text{mon}}=0 \mu\text{V}$ ($T_N=150\text{K}$),
- 2 - pressed $S_{\text{p}}=44\mu\text{V}$ ($T_N=180.5\text{K}$) and

3 – rubbed and pressed $S_{\text{rub,p}}=24.8\mu\text{V}$ ($T_N=180.5\text{K}$). These results indicate that mechanical motions affect the antiferromagnetic phase transition.

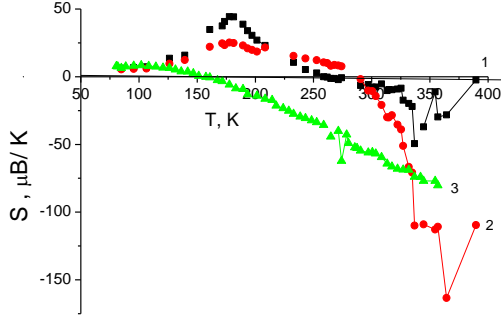


Fig. 6. Thermo-EMF $S(T)$ of samples from temperature dependencies $(\text{TFeS}_2)_{0.975}(\text{TIGaS}_2)_{0.025}$; 1 - single crystal (S_{mon}), 2 – single crystal pressed along the a axis (S_p) and 3 – rubbed and pressed ($S_{\text{rub,p}}$).

At the Neel temperature $\rho(T)$, the resistance has a small break, which is explained by the change in the activation energy of the hopping process. The experimental results show that the conductivity of the TFeS_2 sample at $T < 200\text{K}$ does not depend on temperature. The temperature-independent conductivity may be related to the breakdown of the antiferromagnetic order ($T_N=196\text{K}$) of this crystal.

At $T_N=196\text{K}$, the sign inversion occurs in the $S(T)$ dependence of the compound TFeS_2 . The influence of the Sp-d interaction on the formation of the temperature dependence of thermo-EMF consists of a change of sign and the formation of a negative part in the $S(T)$ dependence at high temperatures. The subsequent increase in temperature leads to the emptying of the lower zone, which was previously completely filled. The latter causes the number of current carriers to increase with holes in a given d-subsystem. At the same time, the number of current carriers in another d-subsystem, whose

energy shifts downward, also increases. Magnetic studies of TlFeS_2 and TlFeSe_2 compounds show an antiferromagnetic phase transition below temperatures of $T_N=196\text{K}$ for TlFeS_2 single crystals and $T_N=290\text{K}$ for TlFeSe_2 . Magnetic susceptibility measurements of TlFeS_2 and TlFeSe_2 single crystals in the temperature range of 2-400 K, which are characteristic of quasi-one-dimensional antiferromagnets showed the behavior. These magnetic studies are in agreement with neutronographic and EPR measurements.

The temperature dependence of electrical conductivity at the value of three-layer solid solution $(\text{TlFeS}_2)_{1-x}(\text{TlGaS}_2)_x$, $x=0.025$ $\sigma(1000/\text{T})$ is characterized by monotonically decreasing activation energy with decreasing temperature. This behavior of conductivity in a solid solution at temperatures of 80÷180K (state of magnetic order) is characteristic of the variable-length hopping mechanism of charge transport, when the current is transferred by charge carriers located in localized states near the Fermi level. In this regard, the temperature dependence of the reconstructed conductance in Mott coordinates $\lg(\sigma)=f(T^{-1/4})$ was also proved.

The density of localized states near the Fermi level was estimated as $N_F=2.9 \times 10^{19} \text{eV}^{-1} \text{cm}^{-3}$. In this case, the value of $a_L=1.4\text{nm}$ was taken from binary GaS for the localization radius. $N_F=1.7 \times 10^{18} \text{eV}^{-1} \text{cm}^{-3}$ for TlFeS_2 . In the studied $(\text{TlFeS}_2)_{1-x}(\text{TlGaS}_2)_x$ samples, the hopping length (R_L) of charge carriers at different temperatures of 80÷180K was calculated. In $\text{TlFe}_{0.975}\text{Ga}_{0.025}\text{S}_2$ at temperatures of 80÷180K $R_{av}=6.2\text{nm}$, the ratio $R_{av}/a_L=4.4$. Note that $R_{av}=10.9\text{nm}$ in TlFeS_2 . For $(\text{TlFeS}_2)_{1-x}(\text{TlGaS}_2)_x$ (where $x=0.025$) solid solution, the energy dispersion of trap states near the Fermi level was $\Delta E=0.07\text{eV}$, and the concentration of deep traps was $N_t=2 \times 10^{18} \text{cm}^{-3}$. (Fig. 7).

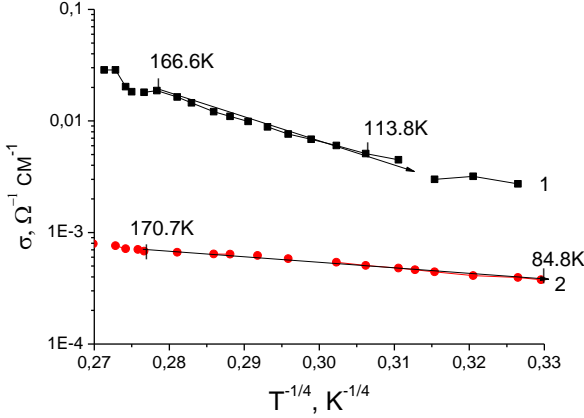


Fig.7. Temperature dependence of the conductivity of the $\text{TlFe}_{0.975}\text{Ga}_{0.025}\text{S}_2$ $\sigma(T^{-1/4})$ sample in the Mott coordinate: 1-single crystal, 2-pressed single crystal.

In the temperature range of 128-178 K, it was determined that the layered single crystal of $(\text{TlFeSe}_2)_{0.5}(\text{TlGaSe}_2)_{0.5}$ solid solution has hopping conductivity in a constant electric field along natural layers. Localized near the Fermi level $N_F=2.8 \times 10^{17} \text{eV}^{-1} \text{cm}^{-3}$ states have variable hopping length conductivity and their dispersion $\Delta E=0.13 \text{eV}$, $R_{\text{av.}}=23.3 \text{nm}$ and concentration of deep traps $N_t=3.6 \times 10^{16} \text{cm}^{-3}$.

In ferromagnets, antiferromagnets, and ferrimagnets, the spins of the atoms and their associated magnetic moments are strictly ordered in the absence of excitation. The excited state of the magnetic system is due to the deviation of the spin from the equilibrium state. Due to the interaction between atoms, such deviation is not localized, but propagates in the form of a wave in the magnetic medium. In the $\rho(T)$ curve of $(\text{TlFeSe}_2)_{0.5}(\text{TlGaSe}_2)_{0.5}$ solid solution at $T_{\text{his}}=109 \div 120$ K, a temperature hysteresis is observed, which is a transition to the incommensurate phase at $T_1 \approx 117.2 \text{K}$ (TlGaSe_2) and $T_C \approx 114 \text{K}$ - is also associated with a proportional phase transition.

It is characterized by a monotonically decreasing activation energy with decreasing temperature in the lower part of the conductivity (σ) $1000/T$ dependence curve. Such conductance

behavior at low temperatures from 80 K to 180 K for sulfur and up to 300 K for selenium in TlFeS_2 , $(\text{TlFeS}_2)_{0.975}(\text{TlGaS}_2)_{0.025}$, and $(\text{TlFeSe}_2)_{0.5}(\text{TlGaSe}_2)_{0.5}$ suggests a charge transport hopping mechanism. In this case, the current is carried by charge carriers localized near the Fermi level. This was also shown by the temperature dependence of the reconstructed conductance in Mott coordinates $\lg \sigma = f(T^{-1/4})$.

The following conclusions can be drawn from the above:

1. We found that the temperature dependence of the reconstructed conductivity $\sigma(T)$ in Mott coordinates $\lg \sigma = f(T^{-1/4})$ of TlFeS_2 can be used to estimate the jump distances at different temperatures. Thus, $R_L = 10.7 \text{ nm}$ at $T = 230 \text{ K}$, $R_L = 11 \text{ nm}$ at $T = 203 \text{ K}$. In the indicated temperature interval, the average jump distance is $R_{av} = 10.9 \text{ nm}$, and the ratio is $R_{av}/a_L = 8$, that is, the average hopping distance significantly exceeds the average distance between charge carrier localization centers. The energy distribution of trap states close to the Fermi level was estimated from the R_{av} values of the TlFeS_2 sample: 1 - $\Delta E = 0.005 \text{ eV}$ and 2 - $\Delta E = 0.007 \text{ eV}$.

2. It is shown that the temperature dependences of electrical conductivity $\sigma(T)$ and thermo-EMF $S(T)$ of TlFeS_2 compound have anomalies. Thus, during the antiferromagnetic phase transition at $T_N = 196 \text{ K}$, a break is observed in the temperature dependences of the electrical conductivity, and in the thermo-EMF dependences, a sign inversion from p-type to n-type is observed.

The calculated magnetic phase transition dissipation energy for pressed TlFeS_2 is 0.129 eV .

3. It was calculated that the tangent of the inclination angle of the dependence established in Mott coordinates in $(\text{TlFeS}_2)_{0.975}(\text{TlGaS}_2)_{0.025}$ solid solution is equal to $T_0 = 2.3 \times 10^6 \text{ K}$, which allows us to estimate the density of localized states near the Fermi level. Localized Fermi states (N_F) are equal to $N_F = 1.7 \times 10^{18} \text{ eV}^{-1} \text{ cm}^{-3}$ for a single crystal and $N_F = 2.9 \times 10^{18} \text{ eV}^{-1} \text{ cm}^{-3}$ for a pressed single crystal. It was calculated that the charge carrier jump length (R_L) of the $(\text{TlFeS}_2)_{0.975}(\text{TlGaS}_2)_{0.025}$ samples studied at different temperatures in the temperature range of $80 \div 180 \text{ K}$ is 6.8 nm at $T = 80 \text{ K}$.

and 5.6nm at T=180K. Thus, the average hopping distance of $(\text{TlFeS}_2)_{0.975}(\text{TlGaS}_2)_{0.025}$ in the temperature range of 80÷180K (antiferromagnetic regularity) was $R_{\text{av}}=6.2$ nm. The value of R_{av} was 4.4 times higher than the ratio of the average distance between the localization centers of charge carriers to the localization radius, that is, $R_{\text{av}}/a_L=4.4$. The value of the activation energy difference between the magnetically ordered and paramagnetic phases, which is 0.106eV and 0.013eV, is the energy spent on the dissolution of the magnetic phase transition of the single crystal and pressed solid solutions $(\text{TlFeS}_2)_{0.975}(\text{TlGaS}_2)_{0.025}$.

4. Thermo-EMF $S(T)$ of $(\text{TlFeS}_2)_{0.975}(\text{TlGaS}_2)_{0.025}$ solid solution is shown in temperature dependence, which undergoes sign inversion from p-type to n-type at $S_{\text{mon}}=0\mu\text{V}$ in a single crystal at $T_N=150\text{K}$. A pressed single crystal at $T_S=255\text{K}$ has $S_p=0\mu\text{V}$ and a pressed single crystal rubbed at $T_S=284\text{K}$ has $S_{\text{rub,p}}=0\mu\text{V}$. These values of Thermo-EMF show that the narrow energy band created by the p-type electrons of the sub-band dissipates with increasing temperature. In the 150÷180K region, the relative temperature dependence of electrical resistances $\rho/\rho_m(T)$ of $(\text{TlFeS}_2)_{0.975}(\text{TlGaS}_2)_{0.025}$ samples: pressed resistance $p/\rho_m(T)$ and rubbed pressed resistance $\rho_{\text{rub,p}}/\rho_m(T)$ have anomalies related to antiferromagnetic phase transition.

5. It was determined that the density of localized states close to the Fermi level was calculated from the temperature dependence of $\lg\sigma=f(T^{-1/4})$ in samples of TlFeSe_2 compound, which was $N_F=3.3 \times 10^{18} \text{eV}^{-1} \text{cm}^{-3}$. The average jump distance in TlFeSe_2 compound was $R_{\text{or}}=10.4\text{nm}$. With the increase of temperature, the thermo-EMF coefficient increased slightly, reached its maximum value at Neel temperature $T_N=290\text{K}$, then decreased to zero at $T=340\text{K}$, after which there was a sign inversion from p-type to n-type. At $T=400\text{K}$, thermo-EMF (S) reaches $-20 \mu\text{V/K}$. The calculated magnetic phase transition breakdown energy for pressed TlFeSe_2 is 0.129 eV.

6. Based on the temperature dependence of electrical conductivity $\lg\sigma=f(T^{-1/4})$ in the layered single crystal of $\text{TlGa}_{0.5}\text{Fe}_{0.5}\text{Se}_2$ solid solution in the range of 128÷178K, it is determined that a variable-length hopping conductance occurs in a constant electric field near

localized states near the Fermi level along its natural layers has been done. Near the Fermi level, the density $N_F=2.8 \times 10^{17} \text{eV}^{-1} \text{cm}^{-3}$, their spread $\Delta E=0.13 \text{eV}$, the average distance of jumps $R_{or}=23.3 \text{nm}$, as well as the concentration of deep traps in this single crystal is $N_t=3.6 \times 10^{16} \text{cm}^{-3}$.

7. It was determined that in the $(\text{TlFeSe}_2)_{0.5}(\text{TlGaSe}_2)_{0.5}$ solid solution, there is a temperature hysteresis in the temperature dependence of the electrical conductivity $\bar{\sigma}(T)$ at the temperature $T_{\text{his}}=109 \div 120 \text{K}$, which indicates that the TlGaSe_2 compound enters the incommensurate phase at $T \approx 117.2 \text{K}$ and at $T_S \approx 114 \text{K}$, it is due to a phase transition to a commensurate magnetoelectric phase.

8. It is shown that the transition inversion of thermo-EMF from p to n-type in temperature dependence of thermo-EMF $S(T)$ of $(\text{TlFeS}_2)_{0.95}(\text{TlGaS}_2)_{0.05}$ antiferromagnet at temperature $T_S=327 \text{K}$ and ρ (at $T_N=190.9 \text{K}$ A break occurs in the dependence of T). Thus, for $(\text{TlFeS}_2)_{0.9}(\text{TlGaS}_2)_{0.1}$ and $(\text{TlFeS}_2)_{0.975}(\text{TlGaS}_2)_{0.025}$ antiferromagnets, thermo-EMF inversion from p-type to n-type at $T_S=150 \text{K}$ and $T_N=$ at $\rho(T)$, respectively breakdown occurs at temperatures of 176.1K and $T_N=150 \text{K}$.

9. It was determined that the sign is positive (p-type) in the thermo-EMF $S(T)$ temperature dependence of $(\text{TlFeS}_2)_{0.975}(\text{TlGaS}_2)_{0.025}$ solid solution from 80K to T_N . This shows that the studied samples have p-type conductivity in the specified temperature range. With increasing temperature, inversion occurs in thermo-EMF for single crystals of solid solution at Neel temperature $T_N=150 \text{K}$. $T_N=180.5 \text{K}$ for a pressed single crystal of this solid solution along the a axis and a rubbed pressed single crystal of the solid solution. The sign inversion of thermo-EMF for pressed and rubbed pressed single crystals occurs at 255K and 284K , respectively. Thermo-EMF up to 355K after Neel temperature of all three samples of $(\text{TlFeS}_2)_{0.975}(\text{TlGaS}_2)_{0.025}$ solid solution is n-type.

In the **fourth chapter**, the results of the research of electrical and thermoelectric properties of low-size TlCrS_2 , TlCrSe_2 , TlCoS_2 , TlCoSe_2 and $(\text{TlGaS}_2)_{0.95}(\text{TlCoS}_2)_{0.05}$ solid solution in the temperature range of $77-400 \text{K}$ were presented.

X-ray analysis of TlCrS_2 and TlCrSe_2 was performed with CuK_α radiation on a DRON-3M diffractometer at room temperature.

The synthesized composition of TlCrS_2 and TlCrSe_2 crystallizes in hexagonal syngony (space group $R3m$). Lattice parameters: for TlCrS_2 $a=0.3538\text{nm}$, $c=2.1962\text{nm}$, $c/a \sim 6.207$, $Z=3$ and $\rho_x=6.705 \text{ g/cm}^3$ and for TlCrSe_2 $a=0.36999\text{nm}$, $c=2.26901\text{nm}$, $c/a 6.133$, $Z =3$ and $\rho_x=6.209 \text{ g/cm}^3$. Electrical properties and thermo-EMF studies of TlCrS_2 and TlCrSe_2 layered compounds in the temperature range of $77\div 400\text{K}$ showed that these compounds have p-type semiconductor character. It became clear that the activation energy for TlCrS_2 in the region of ferromagnetic regularity is $\Delta E_a=0.008\text{eV}$, and $\Delta E_a=0.006\text{eV}$ for TlCrSe_2 . In the paramagnetic temperature region, the activation energy for TlCrS_2 and TlCrSe_2 is $\Delta E_a=0.018\text{eV}$ and $\Delta E_a=0.018\text{eV}$, respectively. These compounds are ferromagnets with Curie temperatures $T_C=125\text{K}$ for TlCrS_2 and $T_C=140\text{K}$ for TlCrSe_2 , and effective magnetic moments $\mu_{\text{eff}}=3.59$ and $\mu_{\text{eff}}=3.71\mu\text{B}$, respectively. The dependence of $\text{Lg}\sigma$ on $T^{-1/4}$ for the TlCrS_2 sample in the temperature range of $80\div 300\text{K}$ is given in Mott coordinates. A graph of temperature dependence of conductivity in $T^{-1/4}$ to $\text{Lg}\sigma$ coordinates was constructed for TlCrS_2 compound in the range of $80\div 190\text{K}$. The value of $T_0=6.3 \times 10^4\text{K}$ was determined from the slope of the dependence of $\text{Lg}\sigma$ on $T^{-1/4}$. From the experimentally found value of T_0 , the density of localized states near the Fermi level in TlCrS_2 $N_F=8.2 \times 10^{19}\text{eV}^{-1}\text{cm}^{-3}$ was determined. In this case, the value of $a_L=3.3\text{nm}$ was taken for the localization radius. The hopping distance in TlCrS_2 crystal at different temperatures was determined. So at $T=80\text{K}$ the value is $R_L=6.6\text{nm}$ and at $T=190\text{K}$ $R_L=5.3\text{nm}$ ie. The average hopping distance (R_{av}) in TlCrS_2 was 6.0nm . The R_{av} value is almost twice as high as the average distance between charge carrier localization centers in TlCrS_2 . After determining the hopping distance at different temperatures (R_L) for the TlCrS_2 compound, we determined the energy distribution of trap states near the Fermi level: $\Delta E=0.027\text{eV}$. It is precisely in the energy band ΔE in the band gap of the TlCrS_2 crystal that charge transfer occurs. At this time, the average value of the activation energy of hoppings in TlCrS_2 determined in the temperature range of $80\div 190\text{K}$ was $\Delta W=0.026\text{eV}$. The concentration

of localized states (N_t) responsible for charge transfer in TlCrS_2 at constant current was also calculated: $N_t = N_F \times \Delta E = 2.2 \times 10^{18} \text{cm}^{-3}$.

The temperature dependence of thermo-EMF in the hopping conductance region of TlCrS_2 crystal was analyzed. The thermo-EMF coefficient of materials in the field of influence of hopping conductivity with variable hopping length ($\log \sigma \sim T^{-1/4}$) can also be characterized by linear asymptotics related to Mott's formula. With increasing temperature, a linear increase in the thermo-EMF coefficient is observed in metallic materials during charge transfer in an energy gap of $k_B T$ close to the Fermi energy (E_F). This is true only if $k_B T \ll E_F$. It follows that the thermo-EMF coefficient at $T=0$ is also zero. In contrast to semiconductor materials, the temperature dependence of the thermo-EMF coefficient (S) in metallic materials in the region of semiconductor hopping conductivity has the form $S(T) = A + BT$ (1), where B is the thermo-EMF temperature coefficient. That is, the extrapolation of the curve $S(T)$ to $T=0$ does not pass through zero. It is also possible that $S(T) \approx \text{const}$ in the hopping region. Thus, from the analysis of theoretical models of thermo-EMF and experimental data, it follows that three types of regularities are possible to describe thermo-EMF in the hopping conduction region: $S(T) \sim T^{1/2}$, $S(T) \sim T$ and $S(T) \approx \text{const}$. These formulas were tested in semiconductors (TiMX_2 , where $M = \text{Fe, Cr}$; $X = \text{S, Se}$) in the study of the thermo-EMF coefficient in the region of hopping charge carrier transfer.

In the temperature dependence of the thermo-EMF $S(T)$ in the TlCrS_2 compound, at low temperatures, hopping charge transport occurs, while the thermo-EMF increases linearly with increasing temperature. The experimental results of the compound TlCrS_2 correspond to the formula (1). The temperature coefficient of thermo-EMF was $B = 0.2 \mu\text{V}/\text{K}^2$. I mean. The low-temperature thermo-EHQ coefficient in TlCrS_2 is determined by the formula $S(T) = (0.2T - 13) \mu\text{V}/\text{K}$.

Synthesis of TlCoS_2 and TlCoSe_2 was carried out by the interaction of primary components with high purity in quartz ampoules created under vacuum up to 10^{-3} Pa pressure. The diffractograms of TlCoS_2 and TlCoSe_2 samples are identical and the

parameters of the elementary core based on hexagonal syngony: for TlCoS_2 $a=0.3726\text{nm}$, $c=2.2510\text{nm}$, $Z=3$ и $\rho=6.026\text{g/cm}^3$ and for TlCoSe_2 $a=0.3747\text{nm}$, $c=2.2472\text{nm}$ and $Z=3$. Due to the large ratio $c/a=6.04$, it can be assumed that TlCoS_2 is a quasi-two-dimensional ferrimagnet.

The temperature dependences of the inverse magnetic susceptibility $\chi^{-1}(T)$ of TlCoS_2 and TlCoSe_2 compounds both have a hyperbolic shape, which is a sign of ferrimagnetism. The paramagnetic Curie temperature (Θ_P) was determined by extrapolating the $\chi^{-1}(T)$ dependence to the temperature axis. The Curie temperature was $T_C \sim 120\text{K}$ for TlCoS_2 and $T_C \sim 75\text{K}$ for TlCoSe_2 . From the $\chi^{-1}(T)$ dependence, the experimental values of the effective magnetic moment were calculated as $\mu_{\text{eff}}=4.6\mu\text{B}$ for TlCoS_2 and $\mu_{\text{eff}}=4.85\mu\text{B}$ for TlCoSe_2 . The theoretical value of the effective magnetic moment calculated taking into account the pure spin value of the trivalent cobalt ion (Co^{3+}) is $4.9\mu\text{B}$. Good agreement is observed between the experimental and theoretical results for TlCoSe_2 . Curie temperatures of $T_C \sim 120\text{K}$ for TlCoS_2 and $T_C \sim 75\text{K}$ for TlCoSe_2 were found from magnetic measurements, which are consistent with literature data.

In order to study the nature of the magnetic phase transition in TlCoS_2 , the heat capacity of this compound was studied. The thermodynamic functions of the solid state (energy, entropy, volume, etc.) remain in continuum when passing through the second type of phase transition point. At the same time, the derivatives of these functions (perceptivity, heat capacity, etc.) undergo a jump at this critical point. For this reason, the maximum of the anomaly in the non-magnetic properties of the magnet, such as the heat capacity, can be used to estimate the state of the magnetic transition. Thus, the small peak in the heat capacity of cobalt-thallium sulfide at a temperature equal to 118K is characteristic of the weak phase transition of the second type corresponding to the Curie point. This maximum is due to the sharp temperature dependence of the magnetization of the ferrimagnet sublattice, at which temperature the collapse of the magnetic order leads to the absorption of the main part of the energy. However, the value of the observed heat capacity anomaly and the

determined magnetic entropy ($\sim 8\text{J}/(\text{mol K})$) in TlCoS_2 are smaller than expected for ferrimagnetic ordering. Presumably, this may be due to the presence of close order in temperature ($T > T_C$). This consists in the maintenance of magnetic order at temperatures above the critical point due to the interaction of spins at close distances. In this case, the exchange forces are sufficient to create regularity at close distances, creating a cluster of ordered spins (magnetization fluctuation).

The entropy of the TlCoS_2 layered ferrimagnet, the small value of the ratio $\Delta S/R=0.02 < \ln 2$, indicates that this phase transition belongs to the second type of displacement transitions.

The temperature dependence of the conductivity of TlCoS_2 and $(\text{TlGaS}_2)_{0.95}(\text{TlCoS}_2)_{0.05}$ solid solution is typical for metals, while semiconducting behavior occurs for TlCoSe_2 . In TlCoS_2 , $(\text{TlGaS}_2)_{0.95}(\text{TlCoS}_2)_{0.05}$ solid solution and TlCoSe_2 compounds, the activation energy in the temperature region with magnetic order is $\Delta E_a = 0.009 \text{ eV}$, $\Delta E_a = 0.002 \text{ eV}$ and $\Delta E_a = 0.005 \text{ eV}$, respectively. The activation energy for these ferrimagnets in the paramagnetic temperature range is $\Delta E_a = 0.116 \text{ eV}$, $\Delta E_a = 0.005 \text{ eV}$ and $\Delta E_a = 0.014 \text{ eV}$, respectively.

The following conclusions can be drawn from the above:

1. It was determined that the activation energies $\Delta E_a=0.008\text{eV}$ for TlCrS_2 and TlCrSe_2 from the temperature dependence of electrical conductivity $\sigma(T)$ were calculated $\Delta E_a=0.006\text{eV}$ in the ferromagnetic magnetic ordered region (before the transition). Also, in the paramagnetic region (after phase transition) $\Delta E_a>0.018\text{eV}$ and $\Delta E_a<0.018\text{eV}$ for TlCrS_2 and TlCrSe_2 , respectively. The calculated breakdown energy of magnetic phase transitions for pressed TlCrS_2 and TlCrSe_2 is 0.01eV and 0.012eV , respectively. For these compounds, the resistivity at 100K is $\rho=134.8\text{Omcm}$ and $\rho=0.1025\text{Omcm}$, and at 300K it is $\rho=48.2\text{Omcm}$ and $\rho=0.1482\text{Omcm}$, respectively.

2. It has been shown that ferromagnets TlCrS_2 ($T_C=116.8\text{K}$) and TlCrSe_2 ($T_C=138\text{K}$) have p-type conductivity in all investigated temperature ranges. These compounds are ferromagnets with Curie temperature $T_C=125\text{K}$ for TlCrS_2 and $T_C=140\text{K}$ for TlCrSe_2 with

effective magnetic moments $\mu_{\text{eff}}=3.59$ and $\mu_{\text{eff}}=3.71\mu\text{B}$, respectively. The theoretical value of the effective magnetic moment calculated taking into account the purely spin value of the trivalent chromium ion (Cr^{+3}) magnetic moment is $3.87\mu\text{B}$.

3. It was shown that the slope of $S(1/T)$ dependence for TlCrS_2 compound in the temperature range of $338\div 370\text{K}$ was $\Delta E_S=0.06\text{eV}$. The activation energy values obtained from the temperature dependence of the thermo-EMF coefficient ($\Delta E_S=0.06\text{eV}$) and electrical conductivity ($\Delta E_G=0.05\text{eV}$) are consistent with each other. While the temperature coefficient of the activation energy of conduction is equal to $\gamma=2.06\times 10^{-4}\text{ eV/K}$, the temperature coefficient of the optical gap (β) in the TlCrS_2 sample is equal to $\beta=2$, $\gamma=4.12\times 10^{-4}\text{ eV/K}$.

4. We determined that the value of $T_0=6.3\times 10^4\text{K}$ found from the temperature dependence of conductivity $\lg\sigma\sim T^{-1/4}$ allows us to calculate the density of localized states near the Fermi level in TlCrS_2 , which is equal to $N_F=8.2\times 10^{19}\text{eV}^{-1}\text{cm}^{-3}$. The hopping distance was determined at different temperatures. The hopping distance at $T=80\text{K}$ is $R_L=6.6\text{nm}$, at $T=190\text{K}$ $R_L=5.3\text{nm}$. Thus, the average hopping distance (R_{av}) in TlCrS_2 is 6.0nm . The R_{av} distance is twice the average distance between charge carrier localization centers in the TlCrS_2 compound.

5. It was determined that the resistance (ρ) of antiferromagnet TlCr_3Se_5 at 100K temperature was 23.65Om cm , and at 300K it was equal to 1.674Om cm . Thermo-EMF of TlCr_3Se_5 compound remained p-type in the entire temperature range. The calculated magnetic phase transition breakdown energy for pressed TlCr_3Se_5 is 0.007eV .

6. It is shown that the resistivity of TlCoS_2 and TlCoSe_2 at 100K temperature is $\rho=0.053\text{Omcm}$ and $\rho=0.0246\text{Omcm}$, and at 300K it is $\rho=0.58\text{Omcm}$ and $\rho=0.0448\text{Omcm}$, respectively. For TlCoS_2 , at a temperature of $T_C=230\text{K}$ ($T_C=109.9\text{K}$), the thermo-EMF sign changes from p-type to n-type. TlCoSe_2 ($T_C=140\text{K}$) n-type ferrimagnet in the entire temperature range. The calculated magnetic phase transition breakdown energy for pressed TlCoS_2 and TlCoSe_2 is 0.007eV and 0.009eV , respectively.

In the **fifth chapter**, the electrical and thermo-EMF properties of TINiS_2 and TINiSe_2 low-dimensional compounds in the temperature range of 77÷400K were discussed.

TINiS_2 and TINiSe_2 samples synthesized by the interaction of highly pure primary elements (Ti, Ni, S and Se) were subjected to X-ray phase analysis. X-ray phase analysis showed that these crystals have hexagonal syngony and lattice parameters: $a=1.228\text{nm}$, $c=1.932\text{nm}$, $\rho=6.900\text{g/cm}^3$ for TINiS_2 and $a=1.260\text{nm}$, $c=1.984\text{nm}$ for TINiSe_2 .

It has been shown that the activation energy of TINiS_2 and TINiSe_2 samples in the temperature range before the metal-dielectric phase transition is $\Delta E_a=0.012\text{eV}$ and $\Delta E_a=0.004\text{eV}$, respectively. In the temperature range after the metal-dielectric phase transition, the values of $\Delta E_a=0.006\text{eV}$ and $\Delta E_a=0.2\text{eV}$ are obtained for TINiS_2 and TINiSe_2 samples, respectively. The specific resistance of TINiS_2 and TINiSe_2 samples at 100K is $\rho=201\text{Om cm}$ and $\rho=0.0032\text{Om cm}$, and at 300K, $\rho=0.25\text{ Ohm cm}$ and $\rho=0.0357\text{Om cm}$, respectively.

In the $\rho(T)$ and $S(T)$ curves of the TINiS_2 samples, the metal-dielectric phase transition at the Curie temperature $T_C=240\text{K}$ occurs with a sharp hop in the electrical resistance $\rho/\rho_{\text{room}} \sim 10^3$ and thermo-EMF $S/S_{\text{room}} \sim 2 \times 10^2$, and the transfer of charge carriers with a hop happens. The observed break in the temperature dependence of $\rho(T)$ of TINiSe_2 at temperature $T_N=120\text{K}$ and the inversion of the thermo-EMF $S(T)$ sign indicate a metal-dielectric phase transition in this compound, which is characteristic of 3d-transition metals.

The following conclusions can be drawn from the above:

1. It was found that the metal-dielectric phase transition in hexagonal TINiS_2 occurs at $T_S=240\text{K}$ and temperatures lower than T_S and is accompanied by a sharp jump in electrical resistance ($\rho/\rho_{\text{room}} > 10^3$). Thermo-EMF $S(T)$ phase occurs at the metal-dielectric phase transition temperature ($S/S_{\text{room}} > 10^2$) and by hopping of charge carriers. From the dependences of the TINiSe_2 sample, the metal-dielectric phase transition is accompanied by a $\rho(T)$ bend at $T_N=120\text{K}$ and an inversion of the thermo-EMF $S(T)$ sign.
2. It is shown that the activation energy of pressed samples of TINiS_2 and TINiSe_2 in the temperature range up to TMD is $\Delta E_a=0.012\text{ eV}$ and

$\Delta E_a=0.004$ eV, respectively. And $\Delta E_a=0.006$ eV and $\Delta E_a=0.2$ eV in the temperature range after the metal-dielectric phase transition for $TlNiS_2$ and $TlNiSe_2$ samples, respectively. The specific resistance of $TlNiS_2$ and $TlNiSe_2$ samples at 100K is $\rho=2010$ m cm and $\rho=0.00320$ m cm, respectively, and at 300K it is $\rho=0.250$ m cm and $\rho=0.03570$ m cm, respectively. The calculated magnetic phase transition breakdown energy for pressed $TlNiS_2$ and $TlNiSe_2$ is 0.006eV and 0.196eV, respectively.

The **sixth chapter** discusses low-dimensional $(TlInSe_2)_{1-x}(TlGaTe_2)_x$ solid solutions. Layered crystals are prototypes of two-dimensional materials in which the ions in the layer are bound by strong covalent and/or ionic bonds, and in the direction of joining the layers, in most cases, the bonding is of Van der Waals character. Such a relatively large difference in the forces of interaction between the elements forming it in the lattice leads to significant anisotropy of the properties, mechanical, electrical, optical, elastic, etc. Below, we will consider experimental data on structural transitions that allow us to understand the reason for the transition and the description of transitions based on Mott's theory.

Samples of $(TlInSe_2)_{1-x}(TlGaTe_2)_x$ solid solutions were obtained by melting stoichiometrically weighed portions of pre-prepared $TlInSe_2$ and $TlGaTe_2$ elementary elements in brazed quartz ampoules under a vacuum of 10^{-3} Pa. To prepare $TlInSe_2$ and $TlGaTe_2$, brands of thallium, indium, gallium Tl-000, In-000, Ga-000, tellurium TB-3 and selenium OST-16⁻⁴ containing no more than 5% additives were used.

$(TlInSe_2)_{0.1}(TlGaTe_2)_{0.9}$, $(TlInSe_2)_{0.2}(TlGaTe_2)_{0.8}$, $(TlInSe_2)_{0.4}(TlGaTe_2)_{0.6}$ and $(TlInSe_2)_{0.6}(TlGaTe_2)_{0.4}$ samples were prepared for electrical measurements at constant current in such a configuration that the external constant let the electric field be directed along the chains of the crystal. Electrodes to the samples were created by electrolytic deposition of copper on the side faces of the crystals. The distance between the electrodes is $L=9$ mm. The intensity of the electric field applied to the crystals corresponds to the ohmic region of the voltammetric characteristic. Temperature dependences of conductivity (σ_{dc}) of $(TlInSe_2)_{1-x}(TlGaTe_2)_x$ (where $x=0.1, 0.2, 0.4$

and 0.6) solid solutions at DC are reconstructed in both Arrhenius coordinates and Mott coordinates. Electrical measurements at direct current cover the temperature range 172–373K.

The $(\text{TlInSe}_2)_{1-x}(\text{TlGaTe}_2)_x$ samples for AC electrical measurements were fabricated in the form of capacitors so that charge transfer occurs along the width of the crystal chains. Silver paste was used as electrodes. The thickness of the crystal is $d \sim 0.45$ mm. Dielectric coefficients of crystals $(\text{TlInSe}_2)_{1-x}(\text{TlGaTe}_2)_x$ were measured by resonance method using TESLA BM 560 coummeter. The frequency range of the alternating electric field is 5kHz÷35MHz. All dielectric measurements were performed at a temperature of 300K. Repeating the resonance condition was ± 0.2 pF on capacitance, $\pm 1.0 \div 1.5$ scale division on Q factor ($Q=1/\text{tg}\delta$). In this case, the biggest deviation from the average values was 3÷4% for ϵ and 7% for $\text{tg}\delta$. Measurements of the physical properties of single crystals of $(\text{TlInSe}_2)_{1-x}(\text{TlGaTe}_2)_x$ solid solutions with a tetragonal structure made it possible to determine the dielectric properties and their frequency dispersion, to determine the nature of dielectric losses and the mechanism of charge transfer in constant and alternating current. The density of localized states and energy dissipation, the average duration and length of jumps, as well as the concentration of deep traps responsible for conduction in direct and alternating current were evaluated. It has been established that in $(\text{TlInSe}_2)_{1-x}(\text{TlGaTe}_2)_x$ solid solutions, hopping conduction occurs in states localized near the Fermi level in constant and alternating current. The dispersion of the dielectric constant in $(\text{TlInSe}_2)_{1-x}(\text{TlGaTe}_2)_x$ has a relaxation character. The hyperbolic drop of the tangent of the dielectric loss angle with increasing frequency from 50 kHz to 35 MHz indicates direct conduction losses in $(\text{TlInSe}_2)_{1-x}(\text{TlGaTe}_2)_x$.

The following conclusions can be drawn from the above:

1. Single crystals of $(\text{TlInSe}_2)_{0.1}(\text{TlGaTe}_2)_{0.9}$ solid solution with tetragonal structure were measured, which made it possible to determine dielectric properties and their frequency dispersion, to determine the nature of dielectric losses. DC and AC charge transfer mechanism, density of localized states and energy dissipation, average

time of crystallization, concentration of deep traps responsible for DC and AC conductivity $(\text{TlInSe}_2)_{0.1}(\text{TlGaTe}_2)_{0.9}$ are evaluated.

It was found that localized charge carriers near the Fermi level occur in direct and alternating current in $(\text{TlInSe}_2)_{0.1}(\text{TlGaTe}_2)_{0.9}$ solid solution with jump conductance. The conductivity dispersion of $(\text{TlInSe}_2)_{0.1}(\text{TlGaTe}_2)_{0.9}$ solid solution has relaxation character.

2. The hyperbolic drop in the dielectric loss tangent with increasing frequency from 50 kHz to 35 MHz shows the loss of conductivity in $(\text{TlInSe}_2)_{0.1}(\text{TlGaTe}_2)_{0.9}$.

3. Crystals of $(\text{TlInSe}_2)_{0.2}(\text{TlGaTe}_2)_{0.8}$ solid solution with tetragonal syngony were grown. In constant electric field $(\text{TlInSe}_2)_{0.2}(\text{TlGaTe}_2)_{0.8}$ crystals, hopping conductivity is observed in localized states close to the Fermi level at temperatures of 100÷175K. The density of states localized near the Fermi level ($N_F=4\times 10^{20}\text{eV}^{-1}\text{cm}^{-3}$) and their energy spread ($\Delta W=0.02\text{eV}$), activation energy ($\Delta E=0.018\text{eV}$) and average hopping distance ($R_{av}=3.7\text{nm}$) are estimated. In low-temperature $(\text{TlInSe}_2)_{0.2}(\text{TlGaTe}_2)_{0.8}$ solid solution, thermo-EMF charge carriers obeyed the regularity $S(T)=(86+1.14T)\mu\text{V/K}$, which is characteristic of the hopping conduction mechanism. With increasing temperature, the thermo-EMF becomes inversely proportional to temperature, when charge carriers excited in the allowed band begin to dominate the conduction. The temperature coefficient of the activation energy of conduction is determined to be $\gamma=1.86\times 10^{-4}\text{eV/K}$.

4. It was determined that during the synthesis of $(\text{TlInSe}_2)_{1-x}(\text{TlGaTe}_2)_x$ (where $x=0.1, 0.2, 0.4$ and 0.6) compositions, tetragonal system solid solutions are formed. The electrical and dielectric properties of the grown chain single crystals in constant and alternating current were studied.

5. It was determined that dielectric losses in $(\text{TlInSe}_2)_{0.4}(\text{TlGaTe}_2)_{0.6}$ samples are related to conductivity. In the frequency range $f=3.2\div 35\text{MHz}$, their alternating current conductivity obeyed the regularity $\sigma_{ac} \sim f^{0.8}$, which is characteristic of the hopping mechanism of charge transport through localized states near the Fermi level.

6. The density (N_F) and energy distribution (ΔE) of these states $N_F=5.8 \times 10^{18} \text{eV}^{-1} \text{cm}^{-3}$, $\Delta E=29 \text{meV}$, average time (τ) and distance (R_L) of hoppings, $\tau=7.4 \times 10^{-8} \text{c}$ is evaluated as and $R_{av}=14.1 \text{nm}$, as well as the concentration of deep traps $N_t=1.7 \times 10^{17} \text{cm}^{-3}$, is responsible for the conductivity of $(\text{TlInSe}_2)_{0.6}(\text{TlGaTe}_2)_{0.4}$ crystals.

7. It was determined that in the temperature range of $291 \div 357 \text{K}$ $(\text{TlInSe}_2)_{0.4}(\text{TlGaTe}_2)_{0.6}$ the thermo-EMF sign is positive, and at $T > 357 \text{K}$ the thermo-EMF sign is inverted, that is, the conductivity of the crystal changes from p-type to n-type.

MAIN RESULTS

1. It was determined that single crystals of $\text{Cu}_{1.22}\text{Fe}_{1.10}\text{Te}_2(\text{a})$ and $\text{Cu}_{1.15}\text{Fe}_{1.23}\text{Te}_2(\text{v})$ grown by gas transport method and $\text{Cu}_{1.13}\text{Fe}_{1.22}\text{Te}_2(\text{b})$ grown by directed crystallization method have a tetragonal structure in chalcopyrite-type compounds. A phase with symmetry $D_{2h}^2=P4/nmm$ is formed. The main parameters of the crystal lattice for CuFeTe_2 (a, b, c) were calculated by radiographic research: $a=0.399 \text{nm}$ and $c=0.617 \text{nm}$ for $\text{Cu}_{1.22}\text{Fe}_{1.10}\text{Te}_2(\text{a})$, $a=0.39749 \text{nm}$ and $c=0.6078$ for $\text{Cu}_{1.04}\text{Fe}_{1.12}\text{Te}_2 \approx \text{Cu}_{1.13}\text{Fe}_{1.22}\text{Te}_2$ and also $a=0.402 \text{nm}$, $c=0.604 \text{nm}$ and $c/a=1.5$ for $\text{Cu}_{1.15}\text{Fe}_{1.23}\text{Te}_2(\text{v})$, vol. $v=0.09745 \text{nm}^3$, density $\rho_{\text{cal}}=6.764 \text{g/cm}^3$ and $\rho_{\text{rentgen}}=6.76 \text{g/cm}^3$.

2. It was determined that below the semiconductor-metal transition temperature (125K) of single crystals of chalcopyrite type $\text{CuFeTe}_2(\text{a, b, c})$ there is a break in the temperature dependence of conductivity $\sigma(T)$. This is explained by the change in the activation energy of the charge transport process with the average hopping length $R_{av} = 2.2 \text{nm}$. At the Neel temperature ($T_N = 65 \text{K}$) and in the spin-glass state ($T_g = 55 \text{K}$), the temperature dependences of $C_p(T)$ and $\chi(T)$ show anomalies related to the antiferromagnetic-paramagnetic phase transition and the spin-glass state. Spin density waves (SDW) are observed above 125K (semiconductor-metal transition temperature) and dissipate near $\sim 300 \text{K}$. From the temperature dependence of magnetic susceptibility (magnetic field $H = 0$) $\chi^{\text{ZFC}}(T)$ and ($H = 1 \text{kOe}$) $\chi^{\text{FC}}(T)$ expansion of magnetic susceptibility is observed, and the point where this temperature dependence intersects is called the closing temperature (T_c). Above the temperature T_c ($T_q > 360 \text{K}$), the

temperature dependence of the magnetic susceptibility $\chi(T)$ changes characteristic of superparamagnets.

3. It was determined that the spin-glass state transition temperature $T_g = 55, 40$ and 35K decreases with an increase in the magnetic field of $1, 10$ and 20 kOe in single crystals of CuFeTe_2 (a, b and c). Effective magnetic moments of paramagnetic clusters have values of $100 \div 1000\text{ Oe } \mu_{\text{eff}} \geq 0.7\mu_B$ in weak field and $10 \div 50\text{ kOe } \mu_{\text{eff}} \sim 2.4\mu_B$ (μ_B – Boron magneton) in strong field. Paramagnetic Curie temperature (Θ_p) is negative.

4. It is shown that the mutual exchange between magnetic "clusters" in CuFeTe_2 (a, b and c) single crystals ($\text{Cu}^+ - \text{Te}^{2-} - \text{Fe}^{3+} = \text{Te}^{2-}$) is antiferromagnetic. In this case, the iron (Fe^{3+}) cation is located between two tellurium (Te^{2-}) anions, and the magnetic moments of the spins are opposite to each other and are arranged parallel to the (001) plane. While CuFeTe_2 single crystals have $Z = 1$ for the crystal structure, it consists of eight formula units - $8(\text{CuFeTe}_2)$ $Z = 8$. The anisotropy coefficient $\eta = 0.309$, three-dimensional Debye temperature $\Theta_D = 176.9\text{K}$ and two-dimensional Debye temperature $\Theta_2 = 122.2\text{K}$ were calculated from the temperature dependence of the heat capacity. .

5. It is shown that in the TlFeS_2 and TlFeSe_2 samples, the hopping conduction with variable length R_L occurs in the region with antiferromagnetic order. The average hopping distance in the temperature range of $80\text{-}180\text{K}$ is $R_{\text{av}} = 10.9\text{ nm}$ and $R_{\text{av}}/a_L > 8$ (a_L -localization radius) for TlFeS_2 and $R_{\text{av}} = 10.4\text{ nm}$ and $R_{\text{av}}/a_L < 8$ for TlFeSe_2 in the range of $85\text{-}250\text{K}$, respectively.

6. It was determined that $(\text{TlFeS}_2)_{0.975}(\text{TlGaS}_2)_{0.025}$ solid solutions have a small refraction at the Neel temperature. The average jump distance $R_{\text{av}} = 6.2\text{ \AA}$ conductance jump of nm occurs. The Neel temperature changes from 150K to 180K when the samples are pressed under pressure $P = 1.5 \times 10^3\text{ kg/cm}^3$.

7. It has been shown that changing the values of $x = 0.025, 0.05, 0.075$ and 0.01 in $(\text{TlFeS}_2)_{1-x}(\text{TlGaS}_2)_x$ solid solutions leads to changes in the Neel temperature and activation energy. It shows the redistribution of gallium (Ga) and iron (Fe) cations in the magnetic structure in the temperature range of $77\text{-}180\text{K}$ in these solid solutions.

8. It was shown that the average hopping length R_{av} along the natural layers of the layered single crystal of the solid solution $(TiFeSe_2)_{0.5}(TiGaSe_2)_{0.5}$ in the temperature range of 128-178 K. = 23.3 nm and $R_{av}/a_L=16$, a breakthrough transmittance occurs. $(TiFeSe_2)_{0.5}(TiGaSe_2)_{0.5}$ This in the temperature dependence of the specific resistance $\rho(T)$ of the solid solution. In the temperature range = 109 - 120 K, temperature hysteresis associated with the proportional and non-proportional phases of $TiGaSe_2$ single crystal is observed.

9. It was determined that $TiCrS_2$ samples have a jump conductivity with an average jump length $R_{av} = 10.9nm$ and $R_{av}/a_L > 8$ in the temperature range of 100-180K. It was determined that the values of $\Delta E_a = 0.009$ eV and $\Delta E_a = 0.005$ eV were calculated for the activation energy of $TiCoS_2$ and $TiCoSe_2$ ferrimagnets in the region of magnetic order. The activation energies in the paramagnetic region for these ferrimagnets are equal to $\Delta E_a = 0.116eV$ and $\Delta E_a = 0.014eV$, respectively.

10. It was determined that $TiNiS_2$ compound has variable hopping conductivity with average length $R_L=3.0nm$ in localized cases near the Fermi level in a constant electric field. It is shown that the metal-dielectric phase transition in the hexagonal $TiNiS_2$ compound occurs at temperature $T_C=240K$, and at a temperature below this temperature, it is accompanied by a sharp hopping of electrical conductivity $\rho/\rho_{room}>10^3$, which is accompanied by the change of conductivity from p-semiconductor to metal. Thermo emf $S(T)$ is $S/S_{room}>10^2$ at metal-dielectric(MD) phase transition temperature. In $TiNiS_2$ crystals, a break in the temperature dependence of the MD phase transition $\rho(T)$ and an inversion of the sign of thermo emf at $T_N=120K$ are observed.

11. It was established that dielectric loss in $(TiInSe_2)_{1-x}(TiGaTe_2)_x$ ($x=0.4$ and 0.6) solid solutions occurs due to direct conduction. In the frequency range $f=3.2\div 35MHz$, the indicated solid solutions obey the regularity of their alternating current conductivity $\sigma_{ac} \sim f^{0.8}$, which is characteristic of the hopping mechanism of charge transfer on localized states near the Fermi level.

DISSERTATION TOPIC PUBLICATIONS

1. Мустафаева, С.Н. Перенос заряда в TlFeS_2 и TlFeSe_2 . С.Н. Мустафаева, Э.М. Керимова, А.И. Джаббарлы. // ФТТ, т.42, 2000, с. 2132– 2135.

2. Алиев, Ф.Ю. Кристаллическая структура и электрические свойства CuFeTe_2 . Ф.Ю. Алиев, Г.Г. Гусейнов, А.И. Джаббаров и С.К. Оруджев. // Физика, т. IV, № 1, 2000, с.58-60.

3. Mustafaeva, S.N. Thermoelectric properties and DC-hopping conductivity of TlMeX_2^6 (Me=Fe, Ni; X=S, Se). S.N. Mustafaeva, E.M. Kerimova, A.I. Jabbarli. / Inorganic Materials Conference, Konstanz, Germany. 7-10 September 2002, Abs. Ref. Number 38.

4. Mustafaeva, S.N. Novel thermoelectric materials on the base of TlGaS_2 - TlCoS_2 . S.N. Mustafaeva, E.M. Kerimova, F.M. Seidov, A.I. Jabbarli. / Abstracts of 13-th International Conference on ternary and multinary Compounds - ICTMC-13, Paris, France. Code number 20 (SO3 A020), October 14 – 18, 2002, P.P. 2-1.

5. Mustafaeva, S.N. Электрические и термоэлектрические свойства TlNiS_2 . S.N. Mustafaeva., E.M. Kerimova., S.İ. Mehdiyeva, А.И. Джаббаров. / International conference on Technical and Physical Problems in Power Engineering, Baku – Azerbaijan, 2002, № 93, p. p. 366-369.

6. Мустафаева, С.Н. Термо-ЭДС в области прыжковой проводимости TlNiS_2 . С.Н. Мустафаева, Э.М. Керимова, А.И. Джаббарлы. // ФТТ, т.45, № 4, 2003, с. 587-589.

7. Выращивание монокристаллов, структурные и магнитные свойства CuFeTe_2 . А.И. Джаббаров, С.К. Оруджев., Г.Г. Гусейнов, Н.Ф. Гахраманов. // Кристаллография, т.49, № 6, 2004, с. 1136-1139.

8. Керимова, Э.М. Температурные зависимости проводимости, термо-ЭДС и теплоемкости TlCoS_2 . Э.М. Керимова, С.Н. Мустафаева, М.А. Алджанов, А.И. Джаббарлы. // Физика низких температур, т. 30, № 4, 2004, с. 395-396.

9. Veliev, R.G. The phase diagram and magneto dielectric properties of the homogeneous phases of TlInS_2 – TlCoS_2 and TlGaSe_2 – TlCoSe_2 systems. R.G Veliev, M.-G.Yu. Seyidov, E.M. Kerimova et ol. // Fizika, cild X, № 1-2, 2004, s. 62-65.

10. Kerimova, E.M. New magnetic semiconductors on the base of $TlB^{VI} - MeB^{VI}$ systems (Me – Fe, Co, Ni, Mn; B – S, Se, Te). E.M. Kerimova, S.N. Mustafaeva, A.I. Jabbarli et al. / *Physics of Spin in Solids: Materials, Methods and Applications*, NATO Sciences; II Mathematics, Physics and Chemistry, v. 156, 2004, p. 195-206.

11. С.К. Оруджов, Магнитные свойства монокристаллов $Cu_{1.22}Fe_{1.1}Te_2$. Оруджов С.К., Гусейнов Г.Г., Джаббаров А.И. и др. // *Изв. НАН Азербайджана*, № 2, 2004, с.104-107.

12. Мустафаева, С.Н Проводимость по локализованным состояниям в монокристалле твердого раствора $TlGa_{0.5}Fe_{0.5}Se_2$. С.Н. Мустафаева, Э.М. Керимова, А.И.Джаббарлы. // *ФТТ*, т. 47, №. 2, 2005, с. 208-209.

13. E.M. Kerimova, Electric conductivity and magnetic susceptibility of $Tl(Cr,Mn,Co)S_2$ layered compounds. E.M. Kerimova, R.G. Veliyev, R.Z. Sadikhov, A.I. Jabbarov. / *TPE – 06 3-rd International Conference on technical and Physical Problems in Power Engineering Turkey*, Ankara., May 29-31, 2006, p. 607- 609.

14. Велиев, Р.Г. Влияние магнитного упорядочения на перенос заряда в слоистых полупроводниковых ферромагнетиках $TlCrS_2$, $TlCrSe_2$. Р.Г. Велиев, Р.З. Садыхов, Э.М. Керимова. // «Физика» №1-2, т. XIII, 2007, s. 260-263.

15. Veliev, R.G.,. State diagram of $TlInS_2 - TlCrS_2$, $TlGaSe_2 - TlCrSe_2$ systems and electric properties of layered compounds $TlCrS_2$, $TlCrSe_2$. R.G. Veliev, F.V.Seyidov, A.I. Jabbarov. // *Fizika* №1, cild XIV, 2008, s. 43-45.

16. Велиев, Р.Г. Рентгенографический анализ, магнитная восприимчивость и электропроводность $TlCoS_2$ и $TlCoSe_2$. Р.Г. Велиев, Э.М. Керимова, Р.З. Садыхов и др. // *Fizika* № 2, cild XV, 2009, s.111-114.

17. Велиев, Р.Г. Магнитные и электрические свойства слоистых магнетиков $Tl(Cr, Mn, Co)Se_2$. Р.Г. Велиев, Р.З. Садыхов, Э.М. Керимова и др. // *ФТП*, т. 43, вып. 2, 2009, с. 163-166.

18. Велиев, Р.Г. Влияние магнитного фазового перехода на перенос заряда в слоистых полупроводниковых

ферромагнетиках TlCrS_2 , TlCrSe_2 . Р.Г. Велиев, Р.З. Садыхов, Э.М. Керимова и др. // ФТП, т. 43, вып. 9, 2009, с. 1175-1178.

19. Велиев, Р.Г. Электрофизические и магнитные свойства слоистых полупроводниковых ферромагнетиков TlCrS_2 , TlCrSe_2 . Р.Г. Велиев, Р.З. Садыхов, Э.М. Керимова и др. // Изв. РАН, серия «Неорган. Материалы», т. 45, вып. 5, 2009, с. 528-533.

20. Керимова, Э.М. Термоэлектрические свойства монокристаллов $(\text{TlInSe}_2)_{0.2}(\text{TlGaTe}_2)_{0.8}$. Э.М. Керимова, С.Н. Мустафаева, А.И. Джаббаров. // Сб. док. IV-ой Международной научной конференции «Актуальные проблемы физики твердого тела ФТТ-2009». Минск. Беларусь. 20 – 23 окт. 2009, т. 2, с. 127-129.

21. Мустафаева, С.Н. Параметры локализованных состояний в твердом растворе $(\text{TlInSe}_2)_{0.1}(\text{TlGaTe}_2)_{0.9}$. С.Н. Мустафаева, Э.М. Керимова, А.И. Джаббаров и др. / Bakı Dövlət universiteti. Fizikanın vüasir problemləri V-ci respublika konfransı “Opto-, nanoelektronika və kondensə olunmuş mühit fizikası” materi. Bakı 16-17 dekabr 2011, s. 85-86.

22. Мустафаева, С.Н. Диэлектрические и термоэлектрические свойства кристаллов на основе исходных соединений системы $\text{TlInSe}_2\text{--TlGaTe}_2$. С.Н. Мустафаева, М.М. Асадов, А.И. Джаббаров, Э.М. Керимова. // Конденсированные среды и межфазные границы, т. 15, № 2, 2013, с. 150–155.

23. Пашаев, А.М. Частотно-зависимые диэлектрические характеристики и термо-ЭДС в кристаллах $(\text{TlInSe}_2)_{1-x}(\text{TlGaTe}_2)_x$. А.М. Пашаев, С.Н. Мустафаева, Э.М. Керимова и др. // Журнал Ученые Записки Национальной Академии Авиации, т. 15, № 1, 2013, с. 18-23.

24. Мустафаева, С.Н. Диэлектрические свойства и перенос заряда в $(\text{TlInSe}_2)_{0.1}(\text{TlGaTe}_2)_{0.9}$ на постоянном и переменном токе. С.Н. Мустафаева, М.М. Асадов, А.И. Джаббаров. // ФТТ, том 56, вып. 6, 2014, с. 1055-1058.

25. Мустафаева, С.Н. Температурная зависимость термо-ЭДС и проводимости твердого раствора $\text{TlFe}_{0.975}\text{Ga}_{0.025}\text{S}_2$ в постоянном электрическом поле. С.Н. Мустафаева, Э.М.

Керимова, А.И. Джаббаров. // Изв. НАН Азербайджана. Сер. Физика и астрономия, т. 34, № 5, 2014, с. 56-60.

26. Мустафаева, С.Н. Перенос носителей заряда в $\text{TlFe}_{0.975}\text{Ga}_{0.025}\text{S}_2$ с участием глубоких локальных центров. С.Н. Мустафаева А.И. Джаббаров. / Труды XVII-ой Международной конференции «Опто-нанoeлектроника, нанотехнологии и микросхемы». Ульяновск, Россия. 15-19 сентября 2014, с. 79-80.

27. Мустафаева, С.Н. Структура и свойства новых функциональных материалов на основе системы $\text{TlFeS}_2 - \text{TlGaS}_2$. С.Н. Мустафаева, Керимова Э.М., А.И. Джаббаров и др. / Тезисы докладов Шестой Международной конференции «Кристаллофизика и деформационное поведение перспективных материалов», посвященной 90-летию со дня рождения проф. Ю.А. Скакова. Москва. 26-28 мая 2015, с. 223.

28. Mustafaeva, S.N. Charge Transport and Thermo-Emf in the $\text{TlFe}_{0.975}\text{Ga}_{0.025}\text{S}_2$ Solid Solution. S.N. Mustafaeva, A.I. Jabbarov / Nineteenth Symposium on Thermophysical Properties, University of Colorado at Boulder, CO, USA. June 21-26, 2015, pp. 272.

29 Мустафаева, С.Н. Проводимость и термо-ЭДС кристаллов $(\text{TlInSe}_2)_{0.2}(\text{TlGaTe}_2)_{0.8}$. Мустафаева С.Н., М.М. Асадов, А.И. Джаббаров, Э.М. Керимова // Неорганические материалы, том 51, № 3, 2015, с. 267-271.

30. Джаббаров, А.И. Магнитные свойства монокристаллов $\text{Cu}_{1.13}\text{Fe}_{1.22}\text{Te}_2$ и $\text{Cu}_{1.15}\text{Fe}_{1.23}\text{Te}_2$ // Azərbaycan Milli Elmlər Akademiyasının Xəbərləri Fizika-texnika və riyaziyyat elmləri seriyası, fizika və astronomiya, cild XXXVII, №5, 2017, s. 31-39.

31. Джаббаров, А.И. Электрические свойства монокристаллов $\text{Cu}_{1.13}\text{Fe}_{1.22}\text{Te}_2$ / Труды международной конференции: «Фундаментальные и прикладные вопросы физики», 13-14 июня Ташкент, т. 2, 2017, с. 44-46.

32. Мустафаева, С.Н. Параметры локализованных состояний и прыжковая термо-ЭДС в TlCrS_2 . С.Н. Мустафаева, С.М. Асадов, А.И. Джаббаров / Восьмая Международная конференция «Кристаллофизика и деформационное поведение перспективных материалов» 5–8 ноября 2019, Москва, с. 162.

33. Мустафаева, С.Н. Прыжковая термо-ЭДС в TlCrS_2 . С.Н. Мустафаева, С.М. Асадов, А.И. Джаббаров // Неорганические материалы, - 2020, том 56, № 4, - с. 351-355.

34. Jabbarov, A.I. Magnetic interaction of “excess” cations Cu^{+2} and Fe^{+2} in the 2D-plane in a single crystal $\text{Cu}_{1.04}\text{Fe}_{1.12}\text{Te}_{1.84}$ // AJP Fizika, 2020, vol. XXVI № 2, pp. 33-37, section: En.

35. Cabbarov, A.İ. $\text{TlFe}_{0.975}\text{Ga}_{0.025}\text{S}_2$ bərk məhlulun nümunənin hazırlanmasından asılı olaraq elektrik və termoelektrik xassələrinin AFM faza keçidinə təsiri // -Bakı: AJP Fizika, - 2022, vol. XXVIII, №1, - s.3-6, section: Az

36. Jabbarov, A. I. Heat capacity and phase transitions in a quasi-duty $\text{Cu}_{1.04}\text{Fe}_{1.12}\text{Te}_{1.84}$ // AJP FIZIKA, 2022, vol. XXVIII, № 1, pp.8-12, section: En

The defense will be held on 16 September 2022 at 11⁰⁰ at the meeting of the Dissertation Council ED 1.14 of Supreme Attestation Commission under the President of the Republic of Azerbaijan operating at Institute of Physics of Azerbaijan National Academy of Sciences.

Address: 131 H. Javid ave., AZ-1143, Baku

Dissertation is accessible at the Library of Institute of Physics of Azerbaijan National Academy of Sciences.

Electronic versions of dissertation and its abstract are available on the official website of the Institute of Physics of Azerbaijan National Academy of Sciences.

Abstract was sent to the required addresses on 12th August 2022

Signed for print: 30.06.2022

Paper format: A5

Volume: 81540

Number of hard copies: 100